APPENDIX D

Mississippi River One-Dimensional Modeling Analysis

TABLE OF CONTENTS

LIST OF TABLES

LIST OF FIGURES

MISSISSIPPI RIVER ONE-DIMENSIONAL MODELING ANALYSIS

1.0 INTRODUCTION

The Mississippi River One-Dimensional Modeling Analysis was completed in support of the Feasibility Study Phase and carried forward into the Preliminary Design Phase for the Riverine Sand Mining / Scofield Island Restoration Project (Project). The Project is sponsored by the Louisiana Department of Natural Resources (LDNR), State of Louisiana Office of Coastal Protection and Restoration (OCPR) and NOAA Fisheries. The Project design is funded and authorized in accordance with the provisions of the Coastal Wetlands Planning, Protection and Restoration Act (CWPPRA) (16 U.S.C.A., Sections 3951-3956) and has been approved by the Public Law 101-646 Task Force. The Project's CWPPRA designation is BA-40.

The primary purpose of the one-dimensional modeling analysis was to evaluate potential impacts to river hydrodynamics from mining the Mississippi River borrow areas which shall serve as the sand sources for restoration of the beach and dune system on Scofield Island as fully described in the Preliminary Design Main Report and Mississippi River Borrow Area Design Analysis (Appendix E). The secondary purpose was to determine if two- or three-dimensional modeling was necessary to fully evaluate the potential impacts.

The scope of services included obtaining existing and acquiring complimentary river hydrodynamic data; setting up, calibrating, and validating the one-dimensional model; predicting changes in river hydrodynamics corresponding to simulated post construction bathymetric surfaces of the excavated borrow areas; and assessing the magnitude of predicted impacts from mining the areas. The modeling analysis was conducted by C.H. Fenstermaker and Associates, Inc. (CHF) and reviewed by SJB Group, LLC. (SJB) and Coastal Engineering Consultants, Inc. (CEC).

2.0 SUMMARY OF PRIOR WORK

The selection of the Project borrow areas was based on the review of prior surveys and analyses that identified multiple areas within the river as containing significant quantities of beach compatible sand. The primary sources of this information included previous geophysical and geotechnical work performed by Coastal Planning and Engineering (CPE, 2004) and Finkl et al. (2005), transport methodology and conveyance corridor analysis (SJB and CEC, 2007a), Mississippi River mining impact assessment (SJB and CHF, 2007), Mississippi River borrow area mining technical analyses (SJB and CEC, 2007b; SJB and CEC, 2007c), previous cultural resources work performed by R. Christopher Goodwin & Associates, Inc. (CGA, 2008), and the Feasibility Study Phase analyses (SJB and CEC, 2008).

CPE (2004) and Finkl et al. (2005) identified potential sand sources within the lower Mississippi River including the two areas designated as MR-B and MR-E. Based on the subsequent surveys and analyses, the boundaries of the two areas were revised multiple times. For the Preliminary Design Phase, these borrow areas have been designated as MR-B-09 and MR-E-09 to reflect that while the approximate locations remained the same, the design limits were refined.

3.0 PROJECT AREA AND LOCATION

Borrow Area MR-B-09 is located on the east side of the Mississippi River near Empire, Plaquemines Parish, between approximate River Mile Marker (MM) 29 to 31, and Borrow Area MR-E-09 is located on the west side of the river south of Buras between approximate MM 23 to 24 as presented in Figure 1.

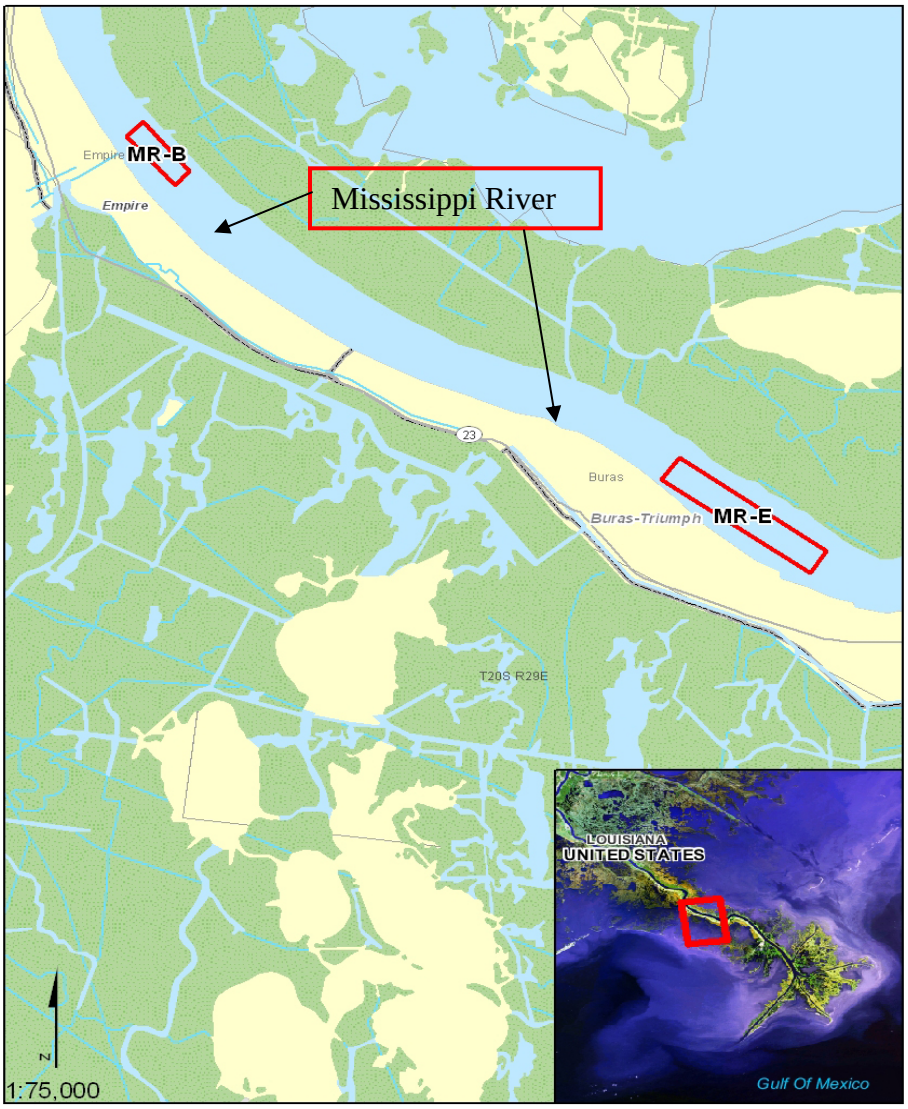

Figure 1: Mississippi River Borrow Area Location Map

4.0 DATA ACQUISITION AND REVIEW

4.1 Available Data

4.1.1 Bathymetry Data

The bathymetric data for the Lower Mississippi River used in this modeling effort were based on the 2003 single-beam survey. The bathymetric data were obtained from the US Army Corps of Engineers (USACE)[1]. The modeling team also used the 2000 LIDAR[2] surveys as well as the US Geological Survey (USGS) Digital Elevation Maps[3] in order to capture the topographic features of the flood plain and to map the levee crests.

4.1.2 Stage Data

Daily and hourly stage data are available at gages operated by USACE in the Lower Mississippi River from Tarbert Landing to the Gulf of Mexico. Table 1 shows the gages in the Lower Mississippi River and Figure 1 shows the location of these gages. Hourly stage data are available only at the following five gages: Red River Landing, Baton Rouge, Reserve, Bonnet Carré and New Orleans. All the other gages record daily stage data. Although historical stage records are available at some locations for as early as 1851, a good set of data exists only after 1950.

4.1.3 Discharge Data

Daily average discharge at Tarbert Landing is available from USACE New Orleans District[4]. Discrete Acoustic Doppler Current Profiler (ADCP) data are available at Bayou Sara (approximately River Mile 270) and Venice. Discrete ADCP data and continuous discharge and water level data are available for Baton Rouge only since 2004. The ADCP data were obtained through direct request to USACE New Orleans District.

[1] http://www.mvn.usace.army.mil/eng2/edsd/misshyd/misshyd.htm
[2] http://atlas.lsu.edu/lidar/
[3] http://www.usgsquads.com/store/moreinfo/EH/moreinfo_EHXLABUNDLE.htm
[4] http://www.mvn.usace.army.mil/eng/edhd/Wcontrol/miss.htm

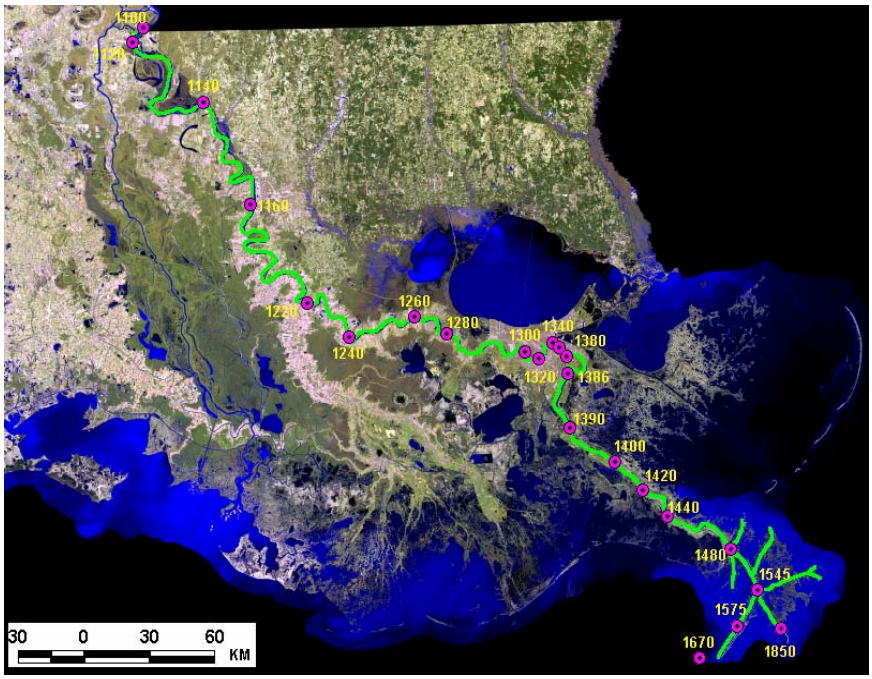

Figure 2: Location of USACE stage gages in the Lower Mississippi River

Table 1: List of USACE gages in the Lower Mississippi

Gage ID	River Mile	Location
1100	306	Mississippi River At Tarbert Landing, MS
1120	302	Mississippi River At Red River Landing, LA
1140	265	Mississippi River At Bayou Sara, LA
1160	228	Mississippi River At Baton Rouge, LA
1220	175	Mississippi River At Donaldsonville, LA
1240	157	Mississippi River At College Point, LA
1260	138	Mississippi River At Reserve, LA
1280	127	Mississippi River At Bonnet Carré, LA
1300	102	Mississippi River At New Orleans (Carrollton), LA
1320	98	Mississippi River (IWW) At Harvey Lock, LA
1340	92	Mississippi River (IWW) At Inner Harbor Navigation Canal Lock, LA
1360	91	Mississippi River At Chalmette, LA
1380	88	Mississippi River (IWW) At Algiers Lock, LA
1386	76	Mississippi River Near Braithwaite, LA
1390	62	Mississippi River At Alliance, LA
1400	48	Mississippi River At West Pointe A La Hache, LA
1420	39	Mississippi River At Port Sulfur, LA
1440	29	Mississippi River At Empire, LA
1480	10	Mississippi River At Venice, LA
1545	0.6	Mississippi River At Head Of Passes, LA
1575	9 DS*	Southwest Pass At Mile 9.2, LA
1670	18 DS	Mississippi River (Southwest Pass) At East Jetty, LA
1850	11 DS	South Pass At Port Eads, LA

*DS: downstream of Head of Passes

4.1.4 Sediment Data

The sediment data at Tarbert Landing, the sole long-term record along the Lower Mississippi River, was used in this numerical modeling effort. The USACE measures and reports daily estimates of the sediment load. The USGS has also measured sediment loads at Belle Chasse. However that site was in operation only from 1977 to 1997. At either location, only the suspended sediment load is reported for the fine and coarse material (diameter smaller and greater than 63 microns, respectively). The coarse material load (sand load) refers to non-cohesive material. The suspended coarse load is virtually non-existent during low flow and increases appreciably during the high flow season. Neither location, Tarbert Landing or Belle Chasse, reports the sediment bed-load transport.

4.2 Data Acquisition

In support of the modeling effort needed to assess the impact of mining sand from the two Borrow Areas MR-B-09 and MR-E-09, additional data was collected at and in the immediate vicinity of the project area. The main purpose of this data collection effort was to ensure that the one-dimensional model would produce reliable results at the project site. In other words, the local flow and sediment parameters were used to refine the model calibration and ensure applicability to the local river reach of interest.

The marine surveying vessel shown in Figure 2 (R/V *Lake Itasca*) was used to collect the field data. The vessel is constructed in typical workboat fashion with a length of 22 feet and an 8 foot-6 inch beam. The vessel has a cabin with dimensions of 7 feet in length, 6 foot- 10 inch width, and 6 foot- 4 inches of headroom. There is ample room for all navigational and data collection equipment inside. The propulsion system is a gas outboard engine with a fuel capacity of 60 US gallons. This vessel belongs to the University of Texas at Austin (UTA). It should be noted that all the sediment analyses were conducted at UTA laboratories. The vessel is equipped with the following:

- Positioning System: A TSS, Inc. POS-MV navigation and orientation system was used throughout the collection of multibeam and sub-bottom data collection. The POS-MV system utilizes a unique Inertially Aided Real-Time Kinematic (IARTK) technology developed by Applanix. The IARTK provides almost instantaneous RTK reacquisition following GPS loss. The POS-MV utilizes enhanced algorithms for robust GPS azimuth measurement and a full six degree-of-freedom position and orientation solution with high update rate.

- Multibeam Echosounder: A Reson, Inc. SeaBat 8101 Multibeam Echosounder was used to measure discrete depths enabling the mapping of the riverbed bathymetry and defining complex underwater features. The SeaBat operates at 240 kHz and 101 transducers that provide a swath-coverage of 150º, enabling a range of about 7.5 times the water depth. Dense coverage with high accuracy is achieved with this instrument by generating up to 40 swath profiles per second (>4000 individual soundings per second). The SeaBat 8101 meets IHO and USACE Class 1 standards.

- Suspended Sediment Sampler: The US P-63 Suspended Sediment Sampler, a point-integrated sampler with an electrically operated valve built by the Federal Interagency Sedimentation Project (FISP), was used for sample collection. The unit is 200 pounds in weight and 37 inches in length with alignment fins to direct the sampler in the direction of travel. Quart or pint (below 100 feet) sample volumes were collected through a 3/16 inch internal diameter intake nozzle. The sampler has the ability to adjust for hydrostatic pressures at the intake nozzle during sampling at flow velocities up to 15 feet per second. Figure 3 shows the US P-63 suspended sediment sampler. At a given cross-section, samples were collected at 0.1, 0.3, 0.5, 0.7, and 0.9 of the total water depths.

(a) (b)

Figure 3: Suspended Sediment Sampler

(a) Picture of the sampler showing the interior collection bottle prior to deployment
(b) Picture of the sampler during the lowering procedure.

- Bathymetry: The survey vessel described above was used to collect high-resolution (multi-beam) bathymetric data at and in the immediate vicinity of the two borrow areas MR-B-09 and MR-E-09. The detailed bathymetry survey was used to estimate the sand bed load. The one-dimensional model is not capable of capturing the effect of the high resolution bathymetry. Therefore, we used the 2003 single beam bathymetry data for the entire one-dimensional model domain.

- Flow and Sediment Data: Two YSI sondes were installed at River Mile 16 and 24.2. These sondes collected water level, salinity, temperature, and turbidity continuously from December 2007 to July 2008. The two stations were surveyed to the vertical datum of North American Vertical Datum of 1998 (NAVD88), and the horizontal datum of North American Datum of 1983 (NAD 83). Time series of the local flow parameters are shown in Figures 4 through 7.

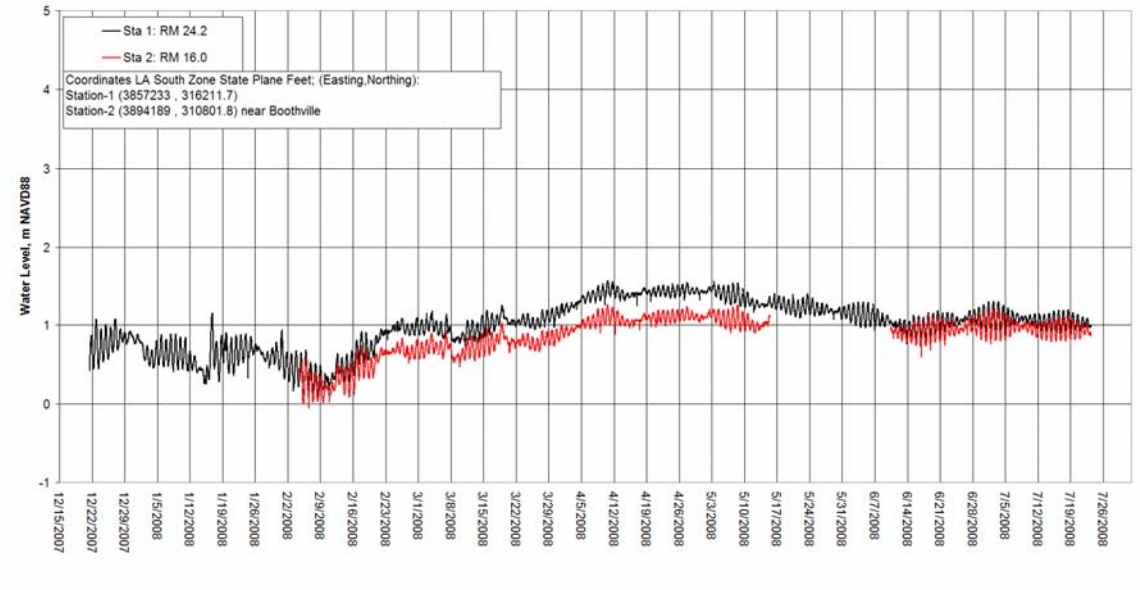

Figure 4: Stage record at the two local monitoring stations

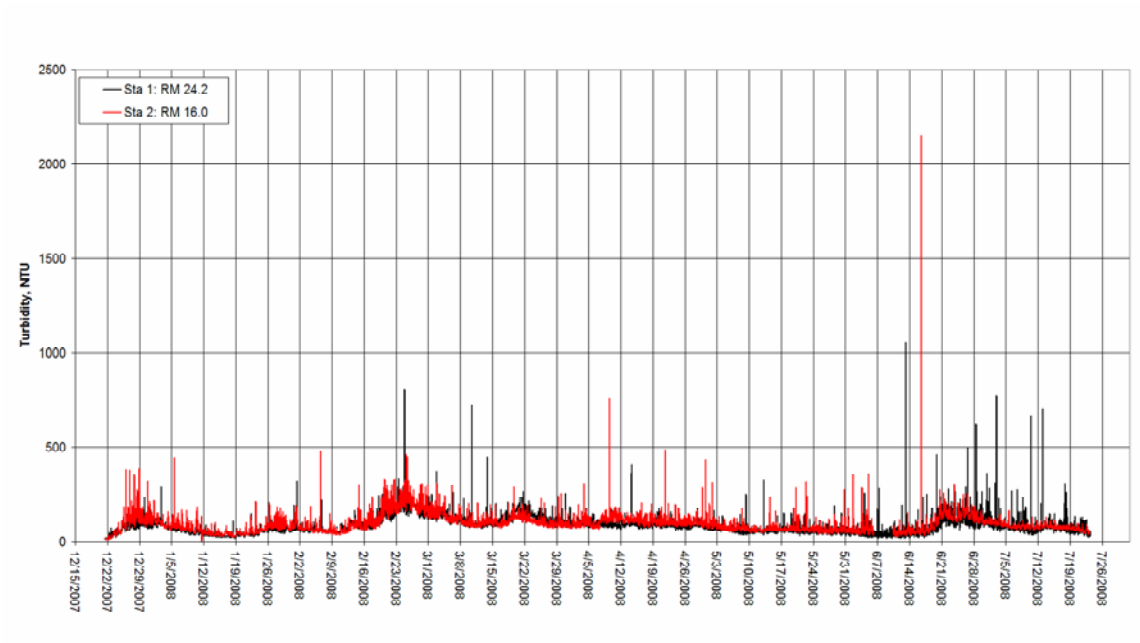

Figure 5: Turbidity record at the two local monitoring stations

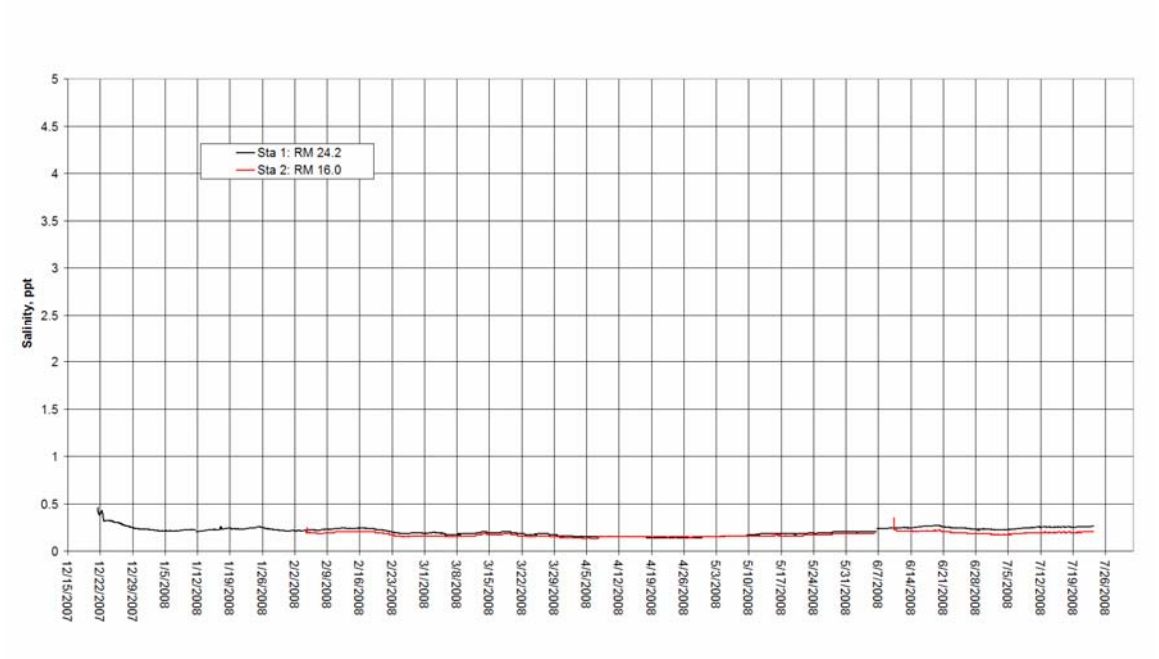

Figure 6: Salinity record at the two local monitoring stations

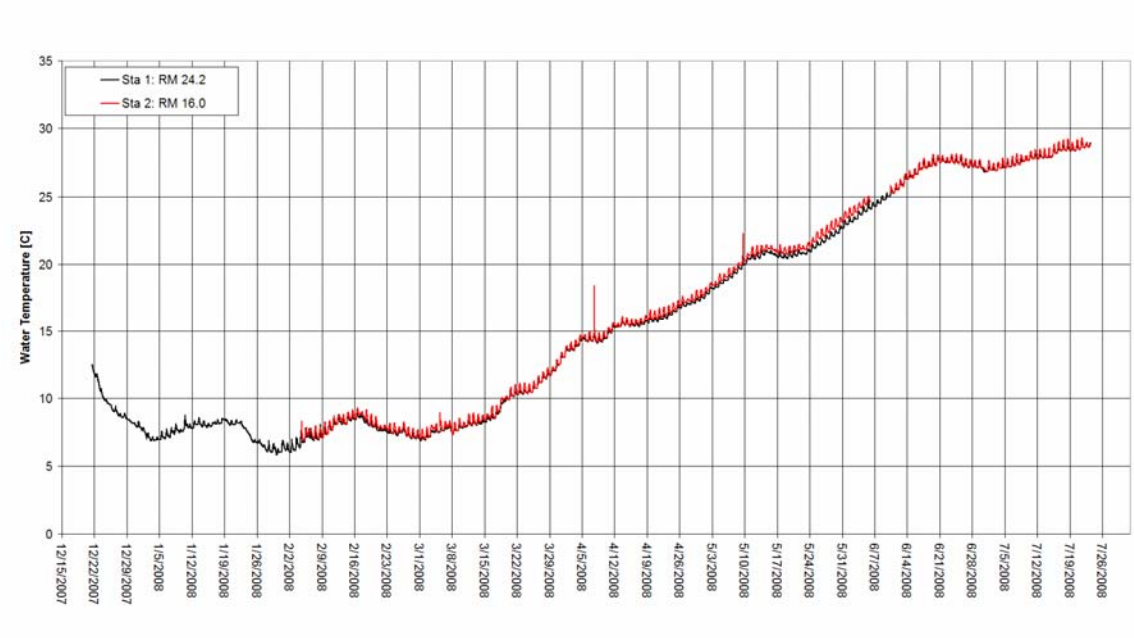

Figure 7: Temperature record at the two local monitoring stations

In addition to the data shown above in Figures 4 through 7, discrete flow and sediment data were collected during two extensive field-data collection trips in January and April of 2008. During these two trips, discrete velocity measurements were collected using an ADCP. Sample of the discrete velocity measurements are shown below in Figures 8 and 9. The ADCP velocity measurements were used to estimate total water discharge using a standard USGS method of

averaging four cross-sections made in immediate succession. Cross-sectional transects were collected along three lines and a grand average utilized for the water discharge reported in Table 2.

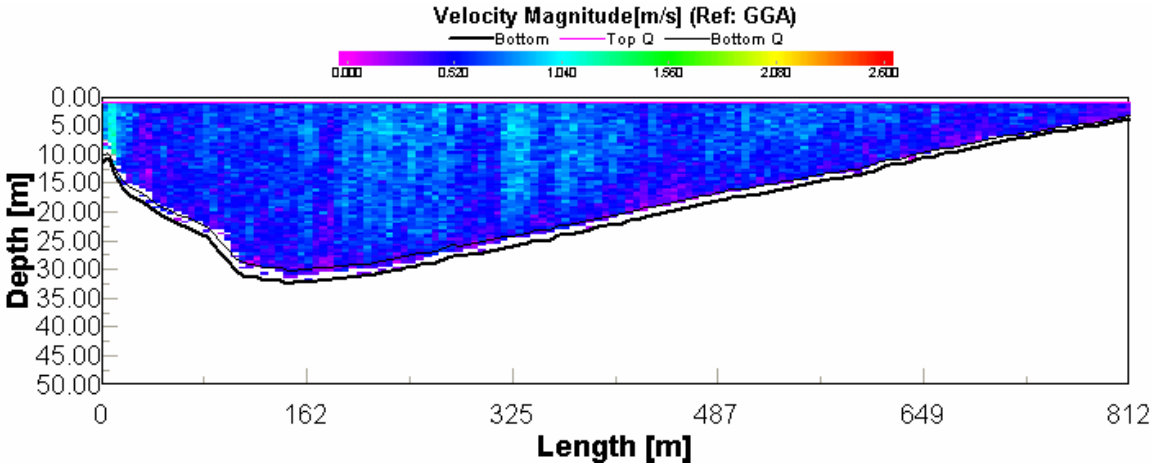

Figure 8: Cross-section sample of the ADCP velocity measurements at MR-B-09, January 2008

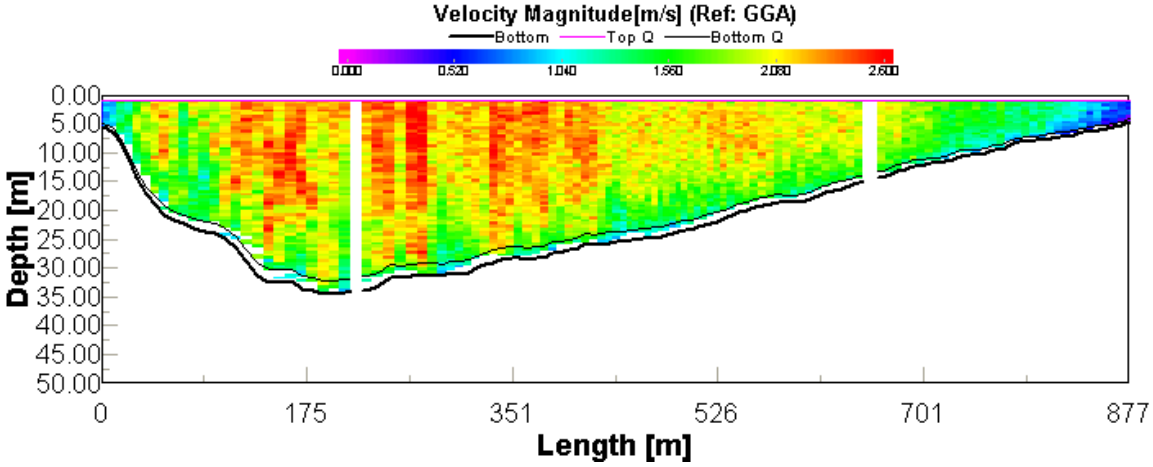

Figure 9: Cross-section sample of the ADCP velocity measurements at MR-B-09, April 2008

Table 2 shows a summary of the discrete flow and sediment measurements during the January and April 2008 trips. Included in the table are the water discharge, sediment bed load, sediment suspended load (for both fine and coarse material), and the total sediment load for coarse material.

Table 2: Summary of the 2008 Lower Mississippi River Flow and Sediment Measurements

	Water Discharge	Bed load	Suspended Load (tons /day)		Sand (Coarse) Load	
	(m^3/s)	(tons /day)	Fine	Coarse	Total (tons /day)	% of sand in suspension
Low Discharge (January 2008)	9,433	2,054	54,730	0	2,054	0
High Discharge (April 2008)	31,592	104,297	634,357	193,845	298,142	65
Ratio	3.3	50.8	11.6	-	145.2	-

5.0 ONE-DIMENSIONAL MODELING

It should be noted that the data collection and modeling analysis was moved up in the schedule of the Project from the Preliminary Design Phase to the feasibility Study Phase. This shift in schedule allowed for the long duration data collection required for the modeling to coincide with the high and low stages of the Mississippi River.. Since refinement of the borrow area perimeters and cut depths would follow the modeling with this advanced schedule, the borrow area dimensions from the Feasibility Study (SJB and CEC, 2008) were used in the analysis. The Feasibility Study delineations of the borrow areas were derived from prior studies and were of a size larger than required for Project construction. It was determined that performing the one-dimensional modeling on a borrow area of larger size than required would provide conservative results.

5.1 Background

The Hydrologic Engineering Center – River Analysis System (HEC-RAS) version 4.0 was used to perform the one-dimensional modeling work. This is a one-dimensional numerical model designed to calculate the water surface and discharge at selected locations along an open channel. It can perform steady and unsteady flow calculations over a fixed bed. Only the recent version of 4.0 incorporates the USACE sediment model HEC-6 (USACE 1993) and is prepared to simulate steady and quasi-steady flows over a mobile-bed. However, not all the options and

capabilities of the original HEC-6 are included in the HEC-RAS version 4.0. Specifically, there are fewer sediment transport/entrainment options available. The sediment load options available in HEC-RAS version 4.0 are:

- Ackers-White
- Engelund-Hansen
- Yang
- Laursen
- Toffaleti
- Wilcock

In addition to these entrainment equations, the following options are available to calculate the sediment settling velocity:

- Toffaleti
- Van Rijn
- Rubey
- Report 12

Detailed information about each of these equations can be found in the HEC-RAS version 4.0 manual (USACE, 2008)

The sediment module of HEC-RAS version 4.0 operates only under a quasi-unsteady mode. The quasi-unsteady mode is an approximation of the fully unsteady flow where a series of steady-state events are simulated consecutively and separated by a constant time interval. This approximation does not include the full dynamic and transient nature of a fully unsteady flow. However, given the fact that the temporal scale of sediment transport is longer than that of water, the quasi-unsteady flow approximation is sufficient to perform long-term (several months to several-years) sediment analysis for the Lower Mississippi River. The series of steady-state events are used to calculate the bed shear-stress which is directly used in the sediment transport equations to determine the sediment load. Once the sediment load is computed, the channel bed is adjusted for erosion or deposition through the sediment mass-conservation equation (known as the Exner Equation).

Although HEC-RAS is a public domain model, the source code is not available. Therefore, the calibration of the sediment module is somewhat limited. Specifically, it is not possible to fine-tune any of the coefficients, parameters and exponents in the various sediment entrainment functions. Thus, the calibration process is limited to the following:

- Selection of the best entrainment option to satisfy observed data

- Selection of the best settling velocity option to satisfy observed data
- Selection of the best erosion/deposition pattern option
- Adjustment of the input temperature and/or grain size distribution (there are obvious constraints on these changes since the inputs data must be consistent with field observations).

5.2 The Model Domain

Two different model domains were used to perform the analysis needed to assess the impact of dredging MR-B-09 or MR-E-09 on the flow and sediment regimes of the Lower Mississippi River. The larger scale model domain extends from Venice at River Mile Marker (MM) 10.7 above Head of Passes to Tarbert Landing at MM 306 above Head of Passes, while the smaller scale model extends from Venice at MM 10.7 to Belle Chasse at MM 76.0 above Head of Passes.

5.3 Model Setup

5.3.1 Channel Geometry

As indicated earlier, the 2003 single-beam survey of the Lower Mississippi River data was used in this modeling effort. A total of 1044 cross-sections of the Mississippi River between Venice and Tarbert Landing were extracted from the field surveys spanning a length of approximately 295 miles. Figure 10 shows a plan view of the large-scale model domain.

5.3.2 Boundary Conditions

The daily hydrographs of water and sediment discharges measured at Tarbert Landing were used as upstream boundary conditions. The daily water stage values measured at Venice were used as downstream boundary condition.

To ensure that the numerical model would provide an accurate assessment of the impact of the dredging operation on the flow and sediment regimes of the river, a thorough calibration process was performed. Several time periods were selected for that purpose. First to calibrate the hydrodynamics, the following two periods were selected: 10/01/1999 to 07/01/2000 and 01/01/2003 to 12/31/2003. Simulations in both unsteady and quasi-unsteady flow modes were performed. To calibrate the sediment transport module, simulations were performed for years 1977/78, 1978/79, 1979/1980, and 1992/1993. The drought period of 10/01/1999 to 07/01/2000 was also used to further calibrate and validate the sediment module through the simulation of the erosion and migration processes of an earthen sill installed by the USACE to prevent saltwater intrusion. The daily hydrographs used as boundary conditions for each modeled period are

presented in Figures 11 through 16, while Tables 3 through 8 show a statistical summary of these boundary conditions.

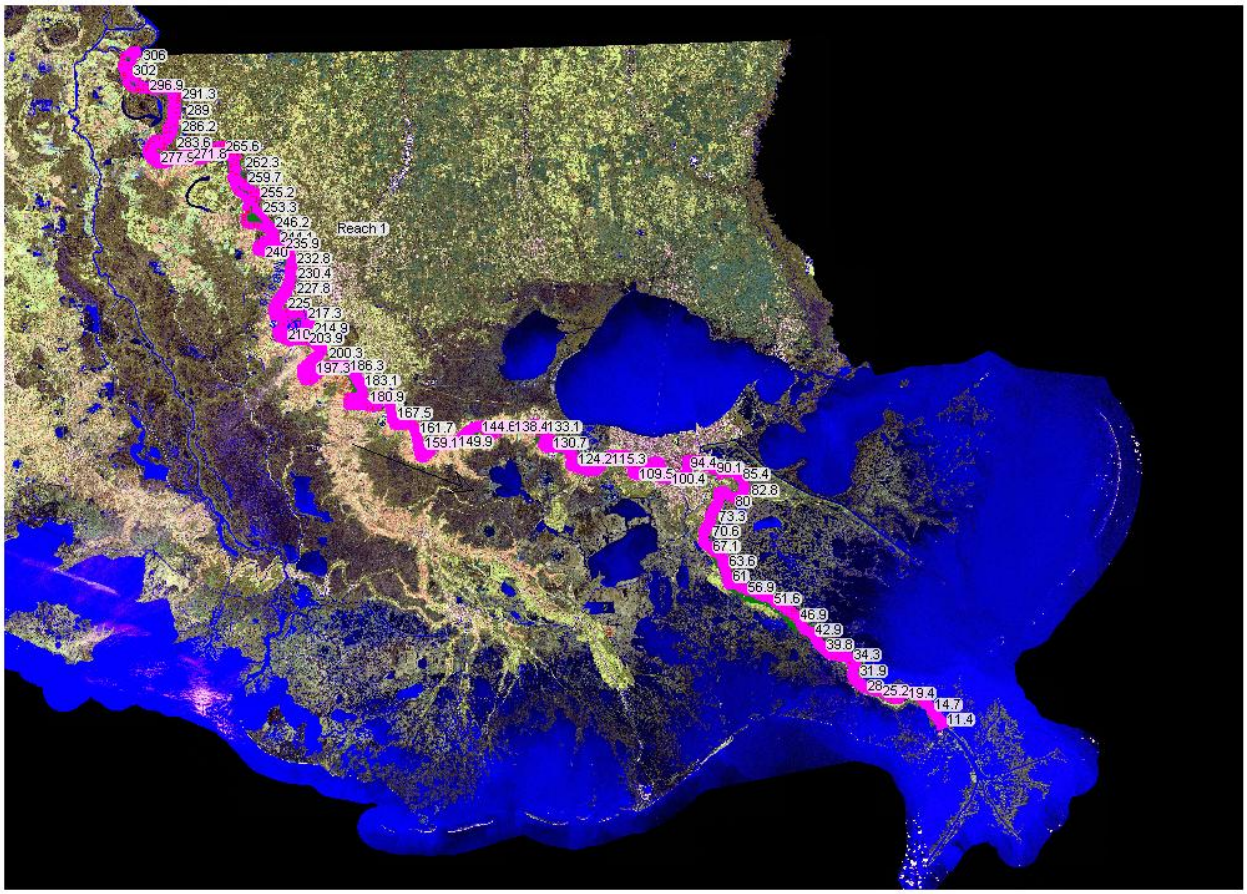

Figure 10: Plan View of the Modeled Reach and Cross-Sections Location

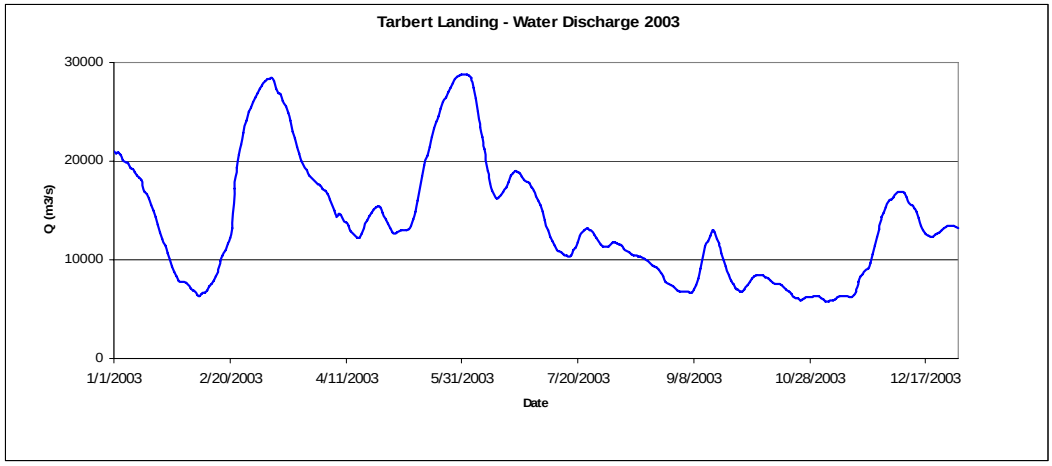

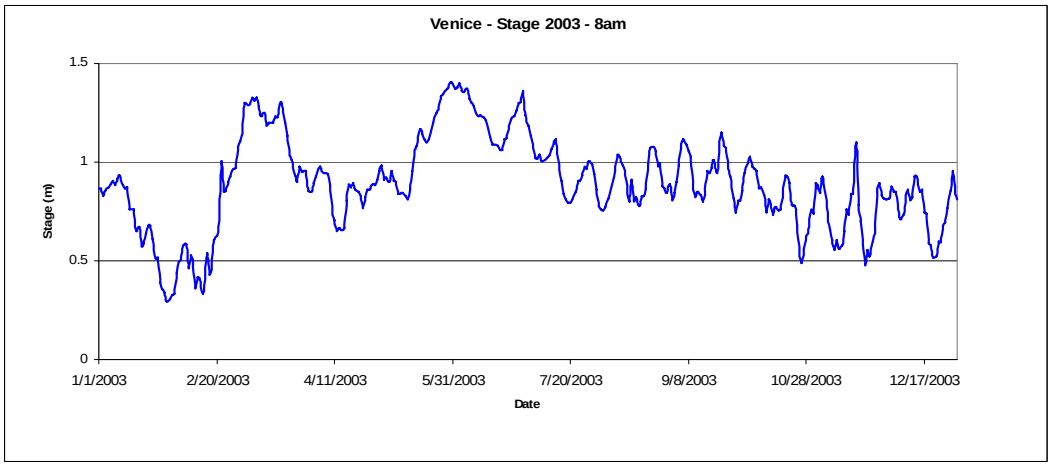

Figure 11: Flow and Stage Hydrographs - 2003 Simulation Boundary Conditions

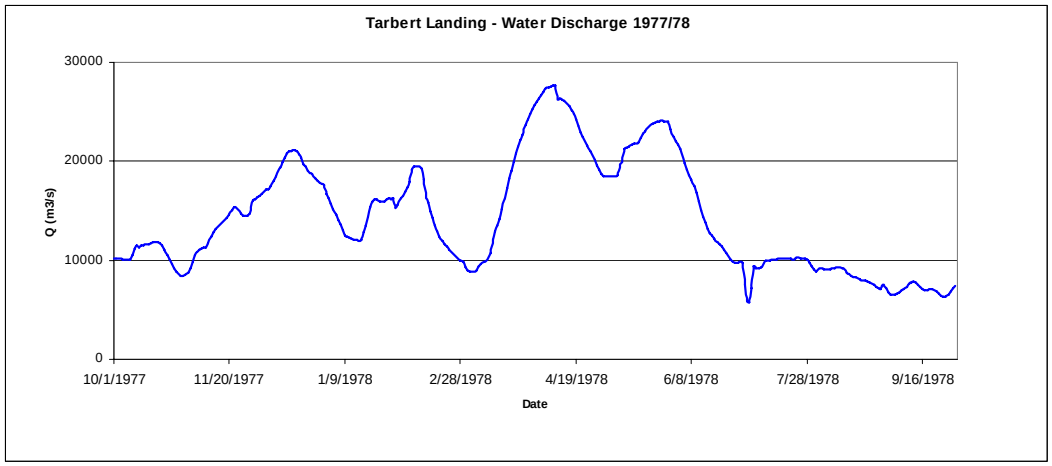

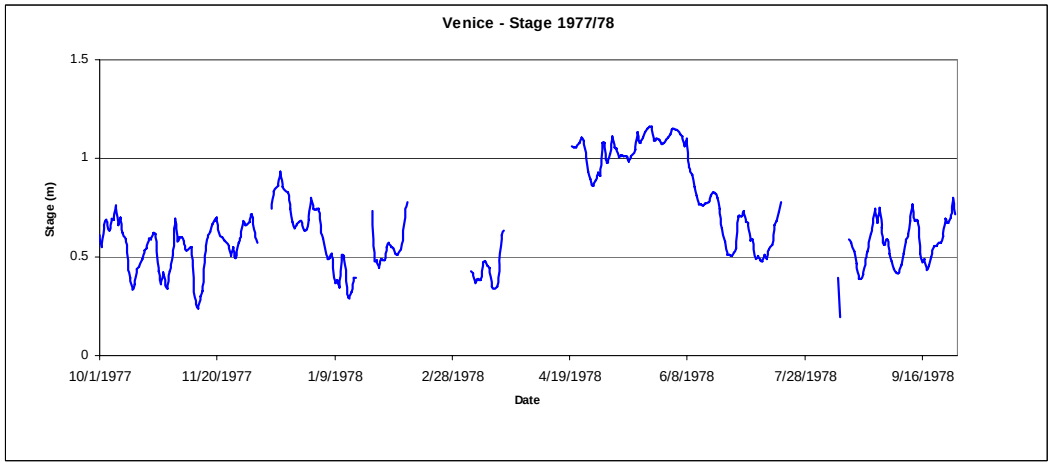

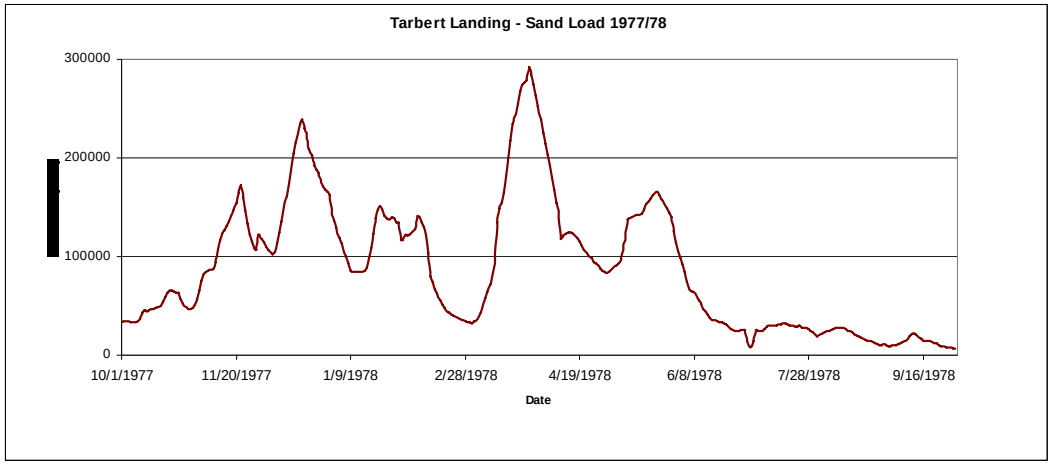

Figure 12: Flow, Stage and Sand Load Hydrographs, 1977/78 Simulation Boundary Conditions.
Note: Sand Load is in tons/day

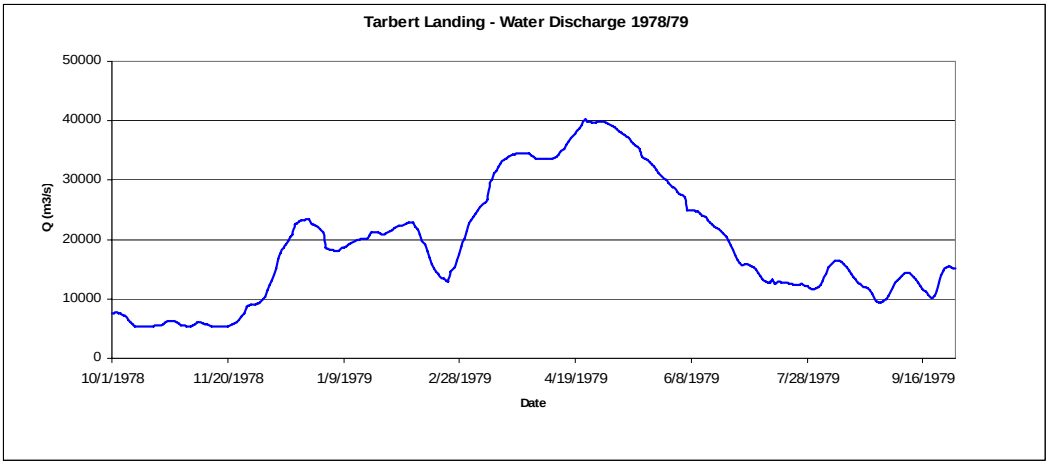

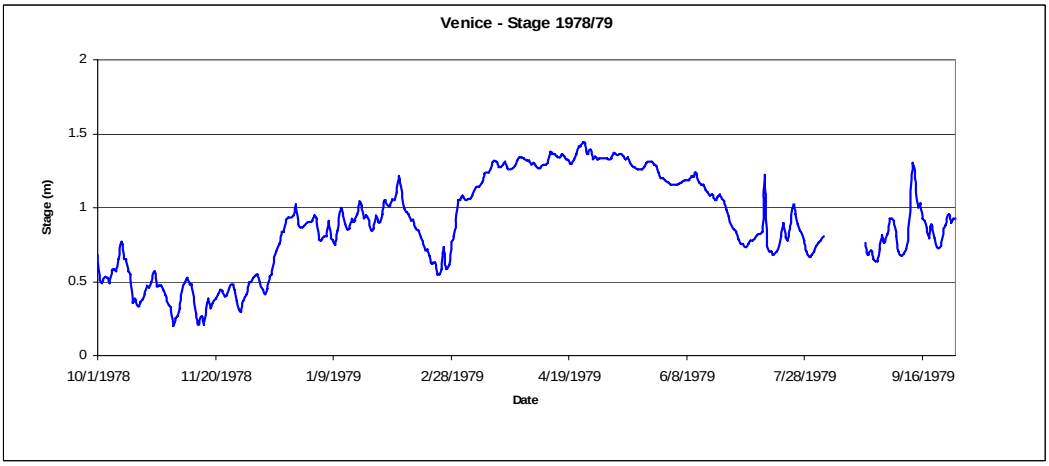

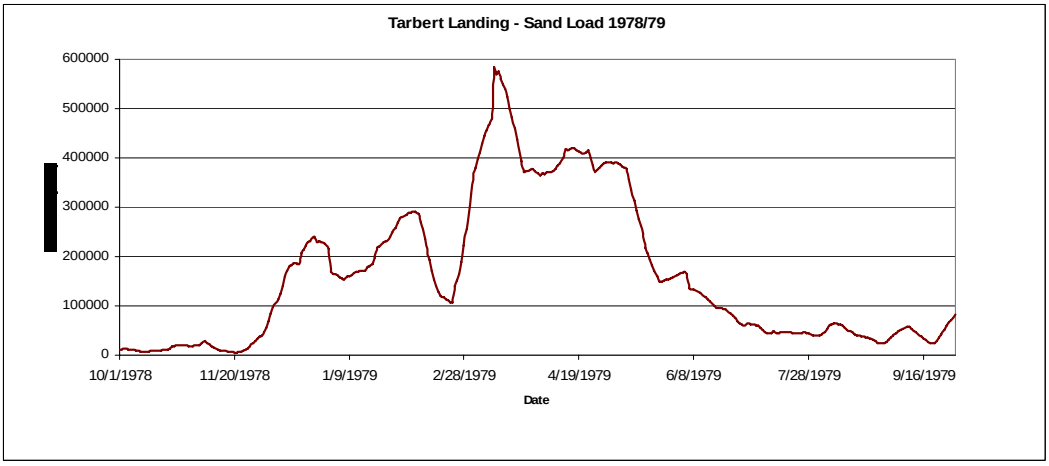

Figure 13: Flow, Stage and Sand Load Hydrographs, 1978/79 Simulation Boundary Conditions.
Note: Sand Load is in tons/day

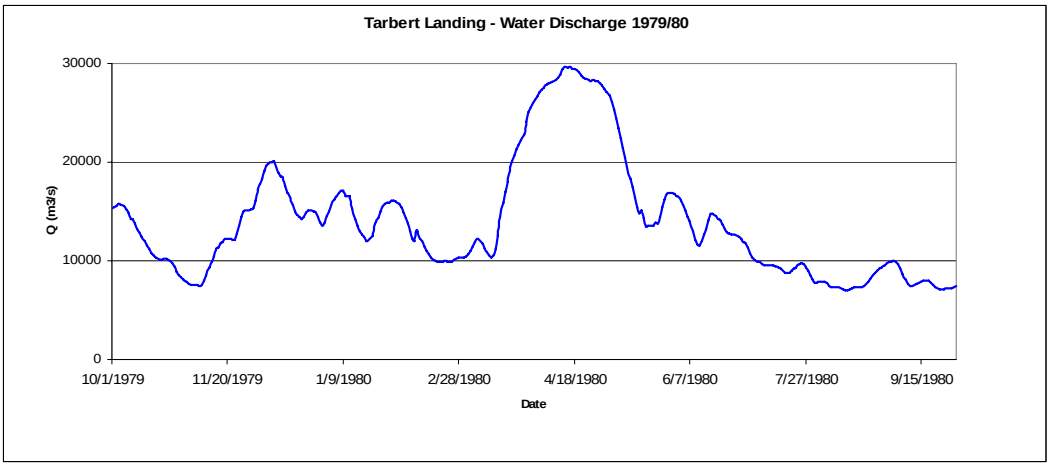

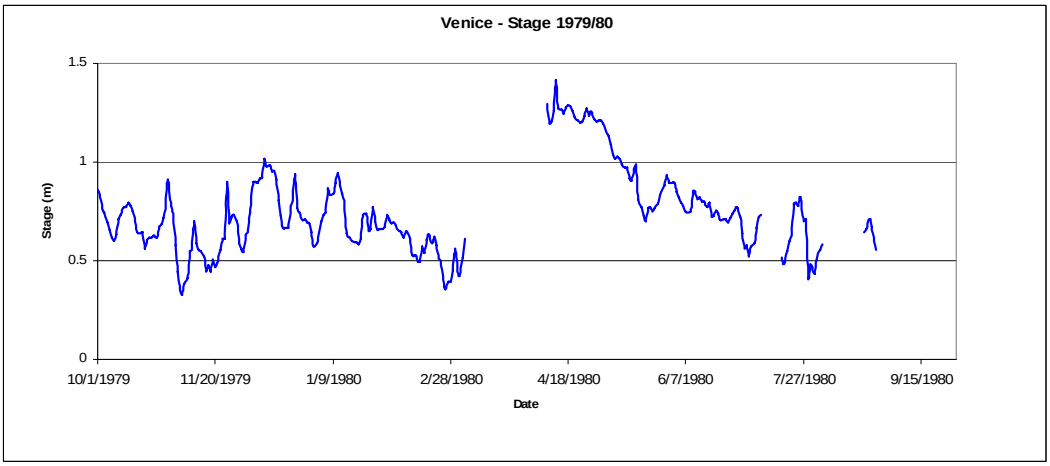

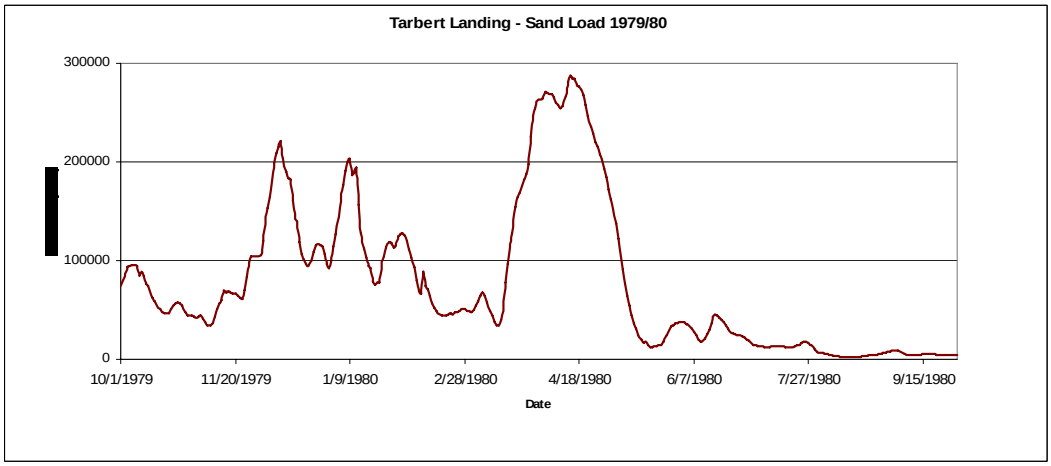

Figure 14: Flow, Stage and Sand Load Hydrographs, 1979/80 Simulation Boundary Conditions.
Note: Sand Load is in tons/day

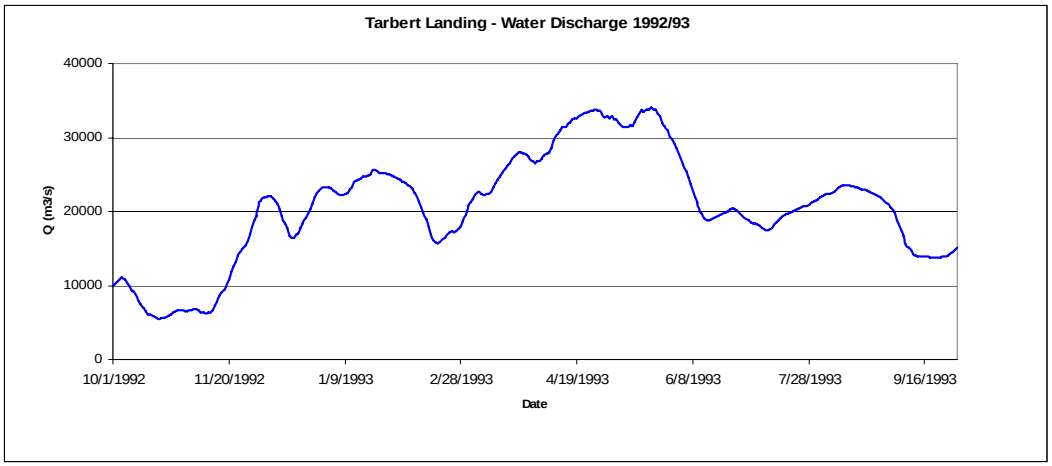

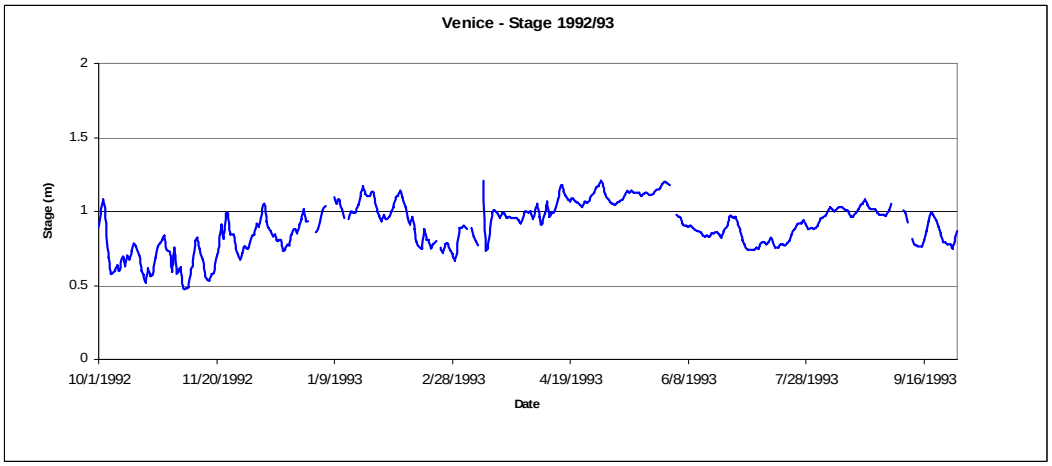

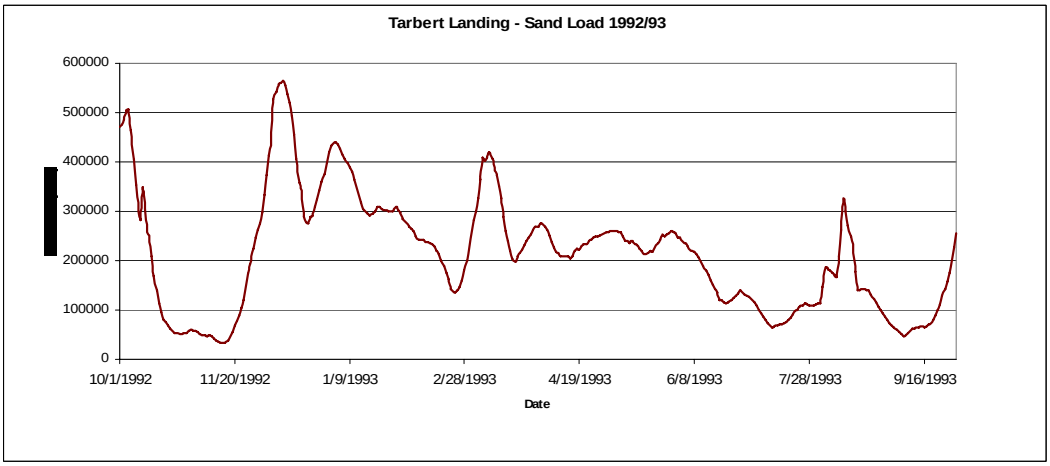

Figure 15: Flow, Stage and Sand Load Hydrographs, 1992/93 Simulation Boundary Conditions.
Note: Sand Load is in tons/day

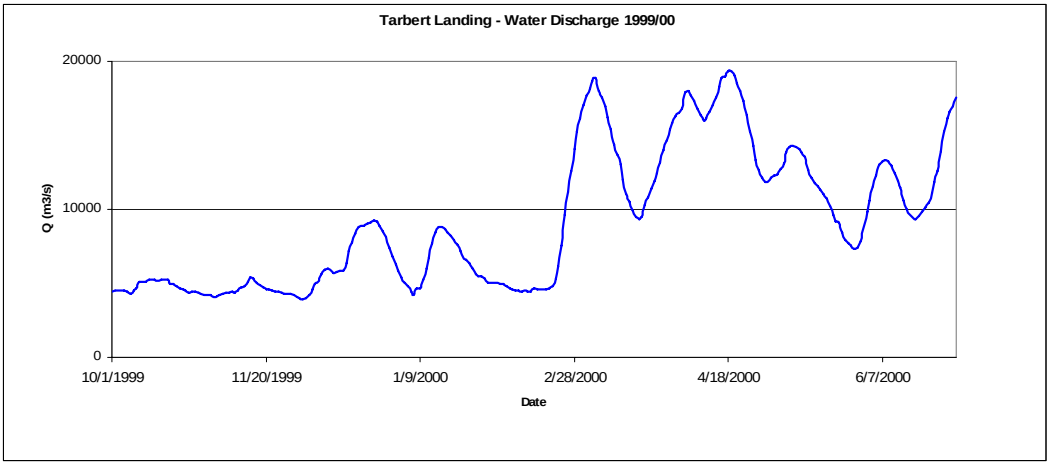

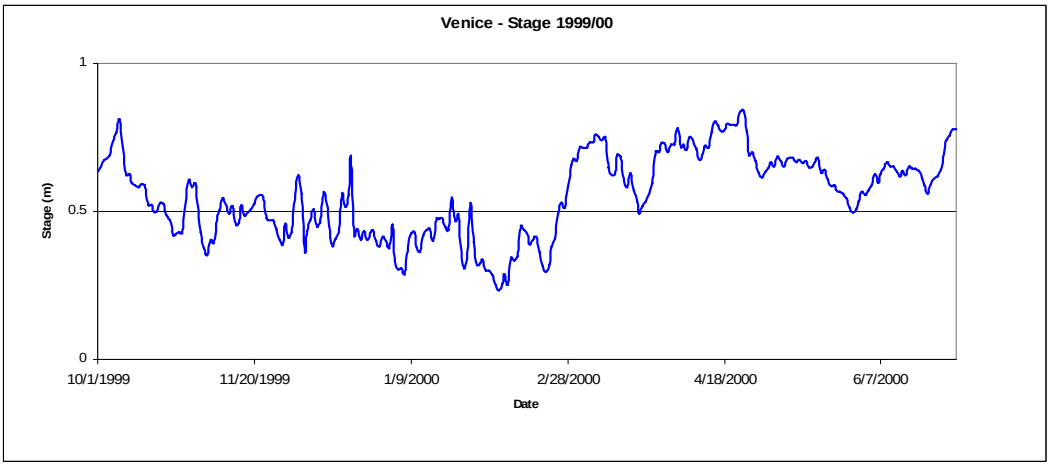

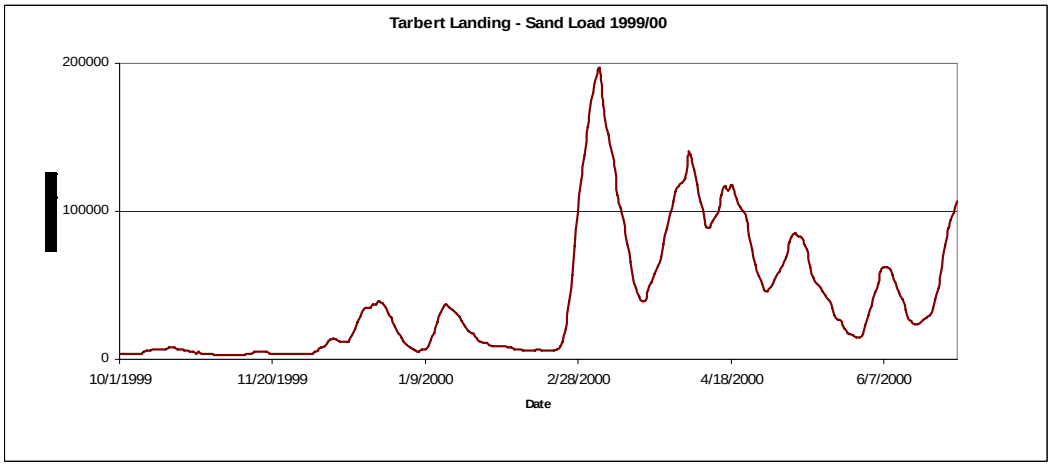

Figure 16: Flow, Stage and Sand Load Hydrographs, 1999/00 Simulation Boundary Conditions.
Note: Sand Load is in tons/day

Table 3: Statistical properties of the hydrographs used for 1977/78 simulations.

Venice 1977/78 - Water Surface Elevation							
Maximum		Minimum		Average		Standard Deviation	
ft	m	ft	m	ft	m	ft	m
3.81	1.16	0.64	0.20	2.18	0.67	0.75	0.23

Tarbert Landing 1977/78 - Water Discharge							
Maximum		Minimum		Average		Standard Deviation	
cfs	m3/s	cfs	m3/s	cfs	m3/s	cfs	m3/s
977,000	27,666	204,000	5,777	505,542	14,315	201,785	5,714

Tarbert Landing 1977/78 - Sand Load			
Maximum	Minimum	Average	Standard Deviation
tons	tons	tons	tons
292,000	7,000	88,326	66,504

Note: Sand Load is in tons/day

Table 4: Statistical properties of the hydrographs used for 1978/79 simulations.

Venice 1978/79 - Water Surface Elevation							
Maximum		Minimum		Average		Standard Deviation	
ft	m	ft	m	ft	m	ft	m
4.75	1.45	0.65	0.20	2.92	0.89	1.04	0.32

Tarbert Landing 1978/79 - Water Discharge							
Maximum		Minimum		Average		Standard Deviation	
cfs	m3/s	cfs	m3/s	cfs	m3/s	cfs	m3/s
1,419,000	40,182	187,000	5,295	679,805	19,250	359,649	10,184

Tarbert Landing 1978/79 - Sand Load			
Maximum	Minimum	Average	Standard Deviation
tons	tons	tons	tons
582,000	5,000	160,945	147,286

Note: Sand Load is in tons/day

Table 5: Statistical properties of the hydrographs used for 1979/80 simulations.

Venice 1979/80 - Water Surface Elevation							
Maximum		Minimum		Average		Standard Deviation	
ft	m	ft	m	ft	m	ft	m
4.65	1.42	1.07	0.33	2.43	0.75	0.71	0.22

Tarbert Landing 1979/80 - Water Discharge							
Maximum		Minimum		Average		Standard Deviation	
cfs	m3/s	cfs	m3/s	cfs	m3/s	cfs	m3/s
1,049,000	29,704	247,000	6,994	493,801	13,983	211,395	5,986

Tarbert Landing 1979/80 - Sand Load			
Maximum	Minimum	Average	Standard Deviation
tons	tons	tons	tons
288,000	2,000	78,290	76,428

Note: Sand Load is in tons/day

Table 6: Statistical properties of the hydrographs used for 1992/93 simulations.

Venice 1992/93 - Water Surface Elevation							
Maximum		Minimum		Average		Standard Deviation	
ft	m	ft	m	ft	m	ft	m
3.97	1.21	1.57	0.48	2.96	0.90	0.52	0.16

Tarbert Landing 1992/93 - Water Discharge							
Maximum		Minimum		Average		Standard Deviation	
cfs	m3/s	cfs	m3/s	cfs	m3/s	cfs	m3/s
1,202,000	34,037	196,000	5,550	729,060	20,645	261,849	7,415

Tarbert Landing 1992/93 - Sand Load			
Maximum	Minimum	Average	Standard Deviation
tons	tons	tons	tons
564,000	33,000	214,208	120,225

Note: Sand Load is in tons/day

Table 7: Statistical properties of the hydrographs used for 1999/00 simulations

Venice 1999/00 - Water Surface Elevation							
Maximum		Minimum		Average		Standard Deviation	
ft	m	ft	m	ft	m	ft	m
2.76	0.84	0.77	0.23	1.81	0.55	0.46	0.14

Tarbert Landing 1999/00 - Water Discharge							
Maximum		Minimum		Average		Standard Deviation	
cfs	m3/s	cfs	m3/s	cfs	m3/s	cfs	m3/s
684,000	19,369	138,000	3,908	324,644	9,193	164,192	4,649

Tarbert Landing 1999/00 - Sand Load			
Maximum	Minimum	Average	Standard Deviation
tons	tons	tons	tons
196,000	3,000	40,858	43,181

Table 8: Statistical properties of the hydrographs used for 2003 simulations

Venice 2003 - Water Surface Elevation							
Maximum		Minimum		Average		Standard Deviation	
ft	m	ft	m	ft	m	ft	m
4.61	1.41	1.56	0.48	3.01	0.92	0.65	0.20

Tarbert Landing 2003 - Water Discharge							
Maximum		Minimum		Average		Standard Deviation	
cfs	m3/s	cfs	m3/s	cfs	m3/s	cfs	m3/s
1,015,000	28,742	205,000	5,805	455,971	12,912	195,787	5,544

5.3.3 Initial Conditions

For all the simulations performed in this analysis, the thalweg line considered by the HEC-RAS model was based on the 2003 survey data. Figure 17 shows the thalweg line used for all the simulations. As seen in the figures, there are deep holes (in the order of 100 feet) at the bottom of the river at several locations. The effect of the turbulent energy created by these 'deep holes' on the transport of bed material is not included in one-dimensional models. The hydrodynamics and turbulence associated with irregular cross-sections were not addressed by the one-dimensional modeling analysis presented herein; however, they are not believed to undermine the integrity of the analysis.

For the simulation of the erosion of the earthen sill for the period 1999 to 2000, additional cross-sections were incorporated into the model to reflect the geometry of the sill as surveyed by the Corps of Engineers. Figure 18 shows a close up of the geometry of the earthen sill.

Spatially variable values of the Manning's "n" roughness coefficient were used. The highest values of the roughness coefficients were used in the upstream portion of the river and the values decreased in the downstream direction. This trend was used to reflect the fact that the bottom material of the Mississippi River gets finer in the downstream direction.

An initial value of the Manning's n roughness coefficient of 0.030 was chosen for the reach between MM 306 and 50.2 above the Head of Passes, and 0.022 for the reach between MM 49.8 to 10.2 above the Head of Passes. The friction coefficient was allowed to vary with the water discharge. Specifically, the correction factors used to adjust the roughness coefficient varied from 0.88 for a flow of 150,000 cfs (4,247 m^3/s) to a value of 0.60 for flows equal or higher than of 1,050,000 cfs (29,733 m^3/s). Fine tuning of the Manning's roughness coefficient took place during the calibration process.

The initial size-class distribution of the sediment bottom material is 20% very fine sand (0.0625 to 0.125 mm), 60% fine sand (0.125 to 0.25 mm) and 20% medium sand (0.25 to 0.5 mm) with an average value 0.194 mm. These values were assumed based on reviews of historical sediment data. This distribution was fine tuned during the calibration process.

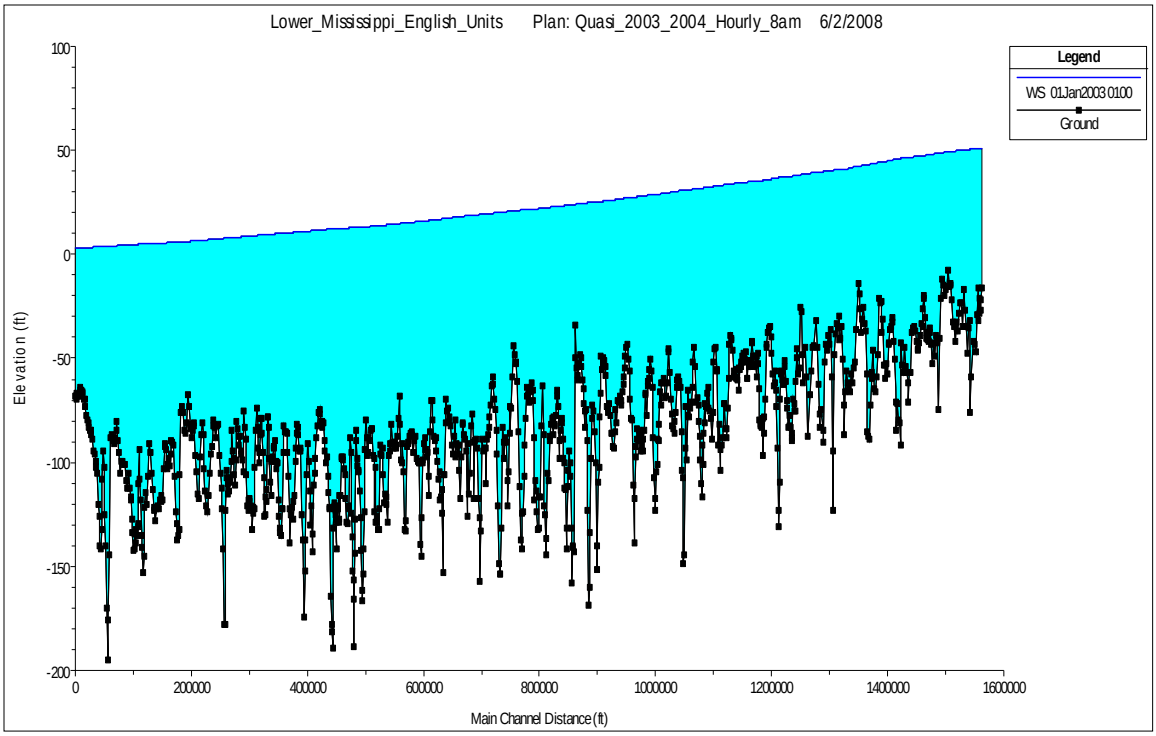

Figure 17: Initial conditions for 2003 simulations

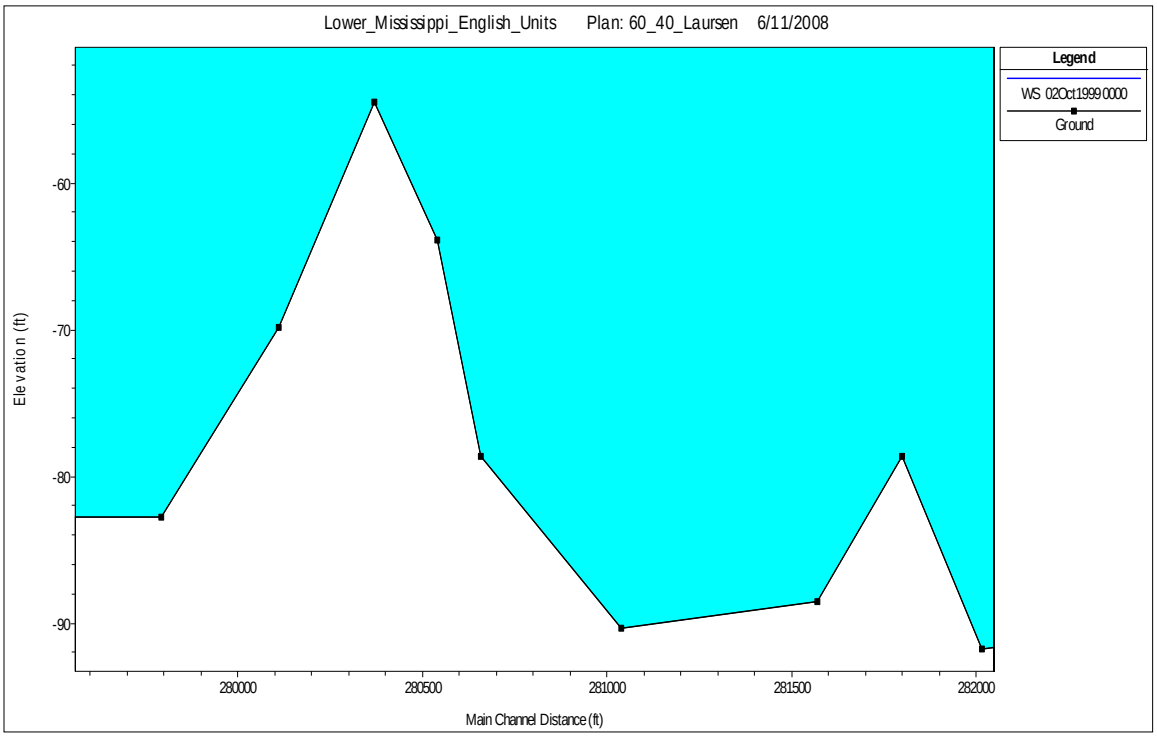

Figure 18: Initial thalweg elevations for the sill cross-sections, 1999/00 mobile-bed simulations

5.3.4 Selection of the Sediment Transport Predictor

As indicated earlier, there are several sediment transport predictors available in the HEC-RAS version 4.0. One of these methods is the Ackers-White (1973) formula. It is a Total-Load predictor. However, it should be used only when $F_r < 0.8$ and is valid in the presence of all types of bed-forms. The Engelund-Hansen (1967) equation is also a total-load predictor. According to Garde and Raju (1985), it does not describe adequately the suspended sediment transport and there is no method to calculate the sediment load per size-fraction. However, the equation is known to provide reasonable results. Both the Ackers-White and Engelund-Hansen formulas are known to be among the predictors that provide better results (Vanoni 1977, White et al. 1973, Alonso 1980, Brownlie 1981 and Neves 1992) (*In* Belo, 1992).

Another method available in HEC-RAS is the Toffaleti method, which is a modified-Einstein total load function that breaks the suspended load distribution into vertical zones, replicating two-dimensional movement (USACE 2002). This method was developed using an exhaustive collection of both flume and field data. The flume experiments used sediment particles with mean diameters ranging from 0.3 to 0.93 mm, however successful applications of the Toffaleti method suggests that a mean particle diameters as low as 0.095 mm are acceptable (USACE 2002). Laursen (1958) formulation is also available in HEC-RAS. This method calculates total-

load. It predicts both the quantity and composition of the sediment in transport (White et al., 1973). Yang's method (1973) is also available and it was developed under the premise that unit stream power is the dominant factor in the determination of total sediment concentration. The research is supported by data obtained in both flumed experiments and field data under a wide range of conditions found in alluvial channels. In 1984 Yang expanded the applicability of his function to include gravel-sized sediments (USACE 2002). These methods were applied to the datasets available in the Mississippi River. A sample of this testing is shown in the next section.

5.4 Model Calibration and Validation

The Manning's n roughness coefficients as well as the adjustment factors (relating Manning's n to the water discharge) were calibrated for the year of 2003 in quasi-unsteady flow mode. Validation was performed for the period of 1999 to 2000. The model was initially calibrated under fully unsteady flow conditions (hydrodynamics only). Afterwards, quasi-unsteady flow simulation was performed to ensure that the model produces realistic water surface profiles in comparison with the field observations. The final Manning's n value of 0.030 was assigned to the reach between miles 306 and 50.2 above the Head of Passes, and a value of 0.022 was assigned to the reach between MM 49.8 and 10.2 above the Head of Passes. The final roughness factors varied from 0.88, for a flow of 150,000 cfs (4,247m^3/s), to a value of 0.60 for flows equal or higher than of 1,050,000 cfs (29,733 m^3/s).

Figures 19 through 23 show a comparison between the observed and simulated water surface elevations at Red River Landing (MM 302.8), Baton Rouge (MM 228.5), Bonnet Carré (MM 127.1), New Orleans/Carrollton (MM 102.8) and West Pointe à La Hache (MM 48.8) for the calibration period. Statistical summary of the model performance is shown in Table 9. Based on the figures and the statistical summary, it was concluded that the model was calibrated properly to enable its use in predicting the affects on river hydrodynamics from mining the borrow areas.

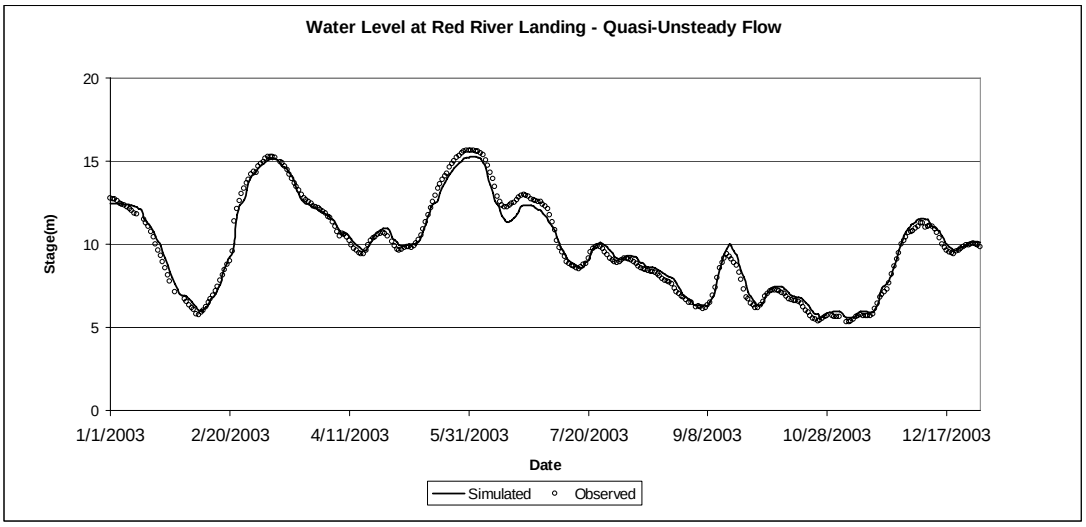

Figure 19: Observed/Simulated Stage at Red River Landing, Quasi-Unsteady Flow 2003

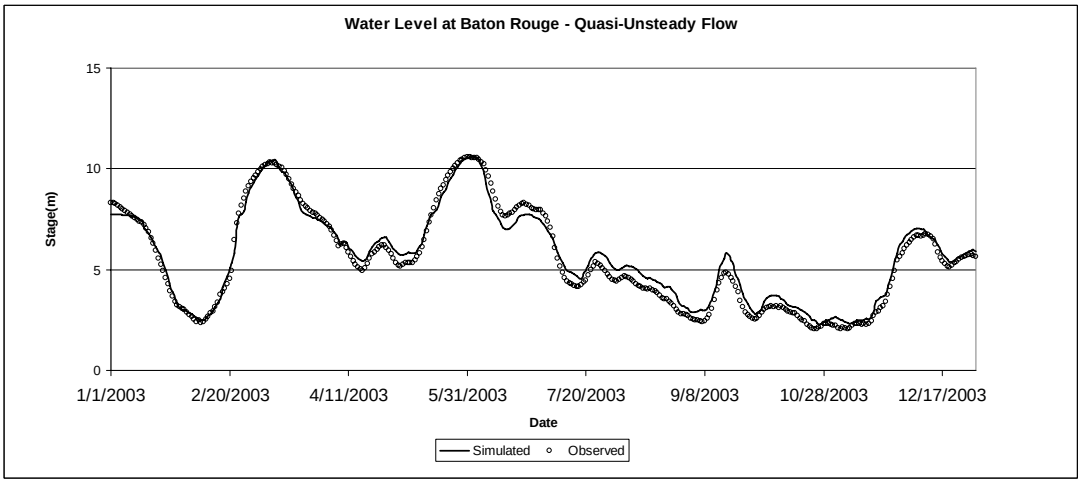

Figure 20: Observed/Simulated Stage at Baton Rouge, Quasi-Unsteady Flow 2003

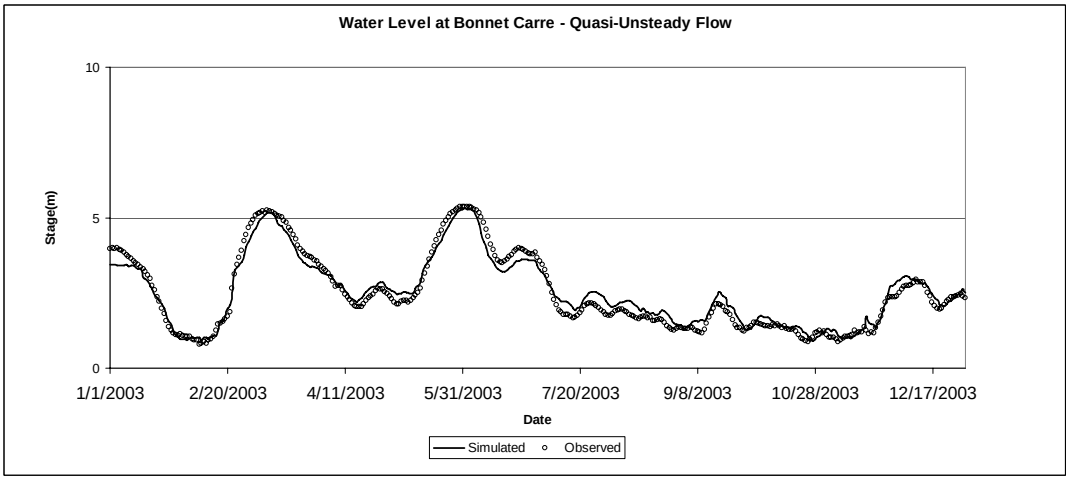

Figure 21: Observed/Simulated Stage at Bonnet Carré, Quasi-Unsteady Flow 2003

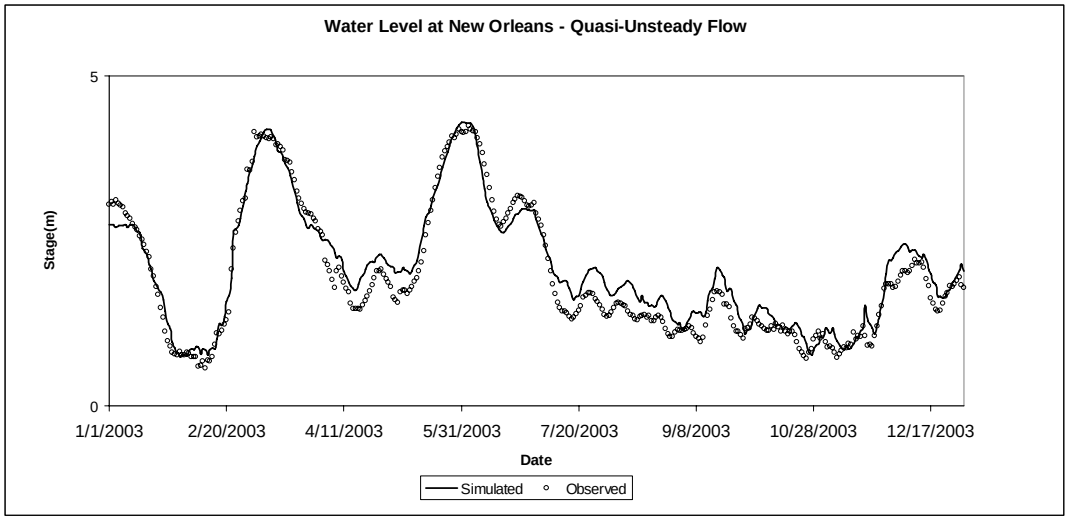

Figure 22: Observed/Simulated at New Orleans, Quasi-Unsteady Flow 2003

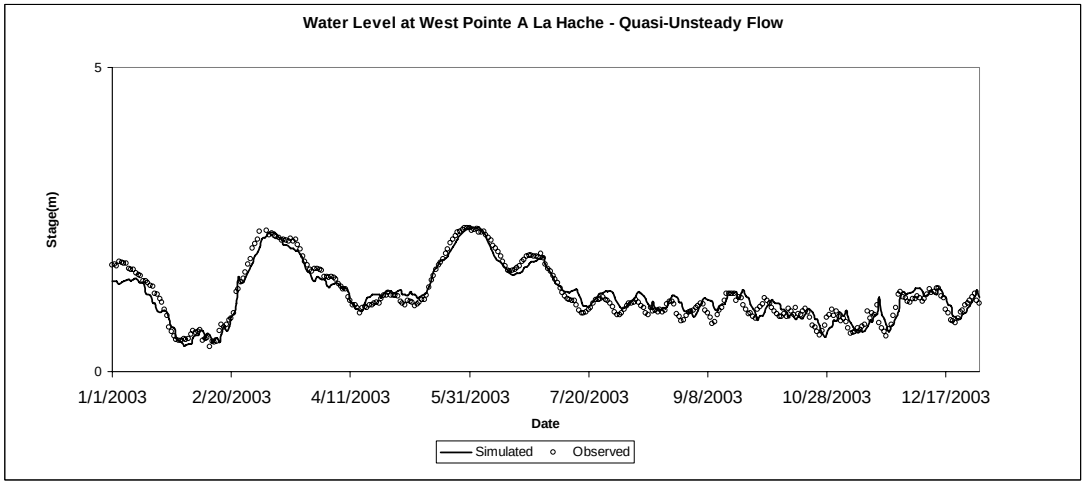

Figure 23: Observed/Simulated Stage at Pointe a La Hache, Quasi-Unsteady Flow 2003

Table 9: Statistical summary of the model performance for the calibration period

Location	RMSE (m)	Efficiency
Mississippi River at Red River Landing	0.311	0.994
Mississippi River at Baton Rouge	0.420	0.980
Mississippi River at Bonnet Carre	0.265	0.968
Mississippi River at New Orleans	0.247	0.954
Mississippi River at West Pointe A La Hache	0.133	0.948

A second independent simulation for the years of 1999 and 2000 was performed without any further adjustments to the hydrodynamic model parameters to fully assess the model performance. Figures 24 to 27 show a comparison between the observed and simulated water surface elevations at Red River Landing (MM 302.8), Baton Rouge (MM 228.5), Bonnet Carré (MM 127.1) and West Pointe a La Hache (MM 48.8) for the validation period of 1999/00.

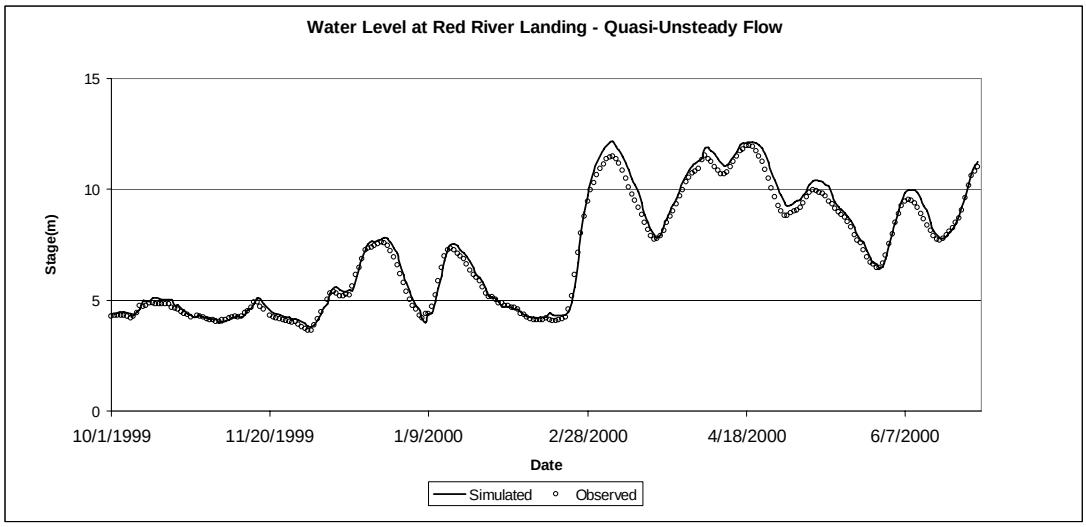

Figure 24: Observed/Simulated Stage at Red River Landing, Quasi-Unsteady Flow 1999/00

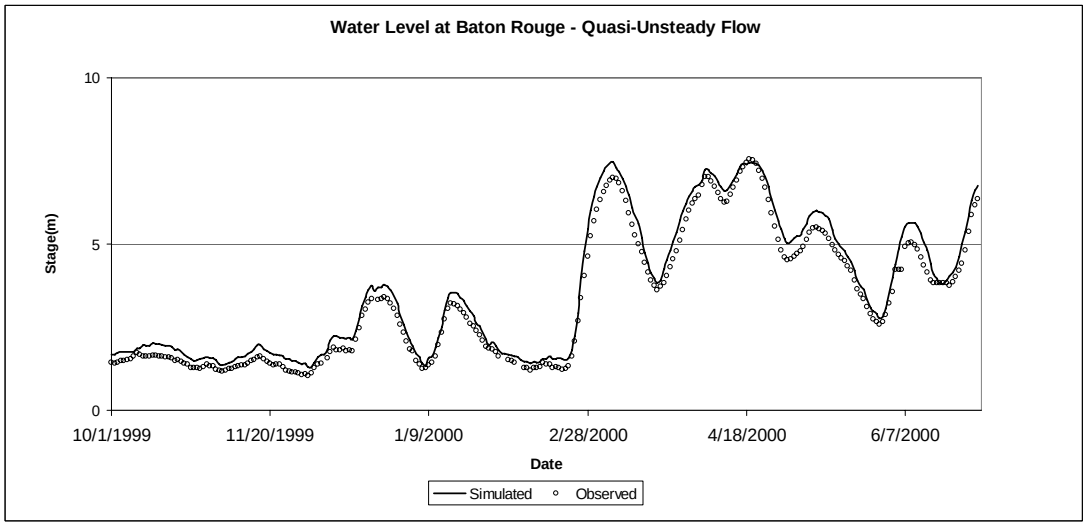

Figure 25: Observed/Simulated Stage at Baton Rouge, Quasi-Unsteady Flow 1999/00

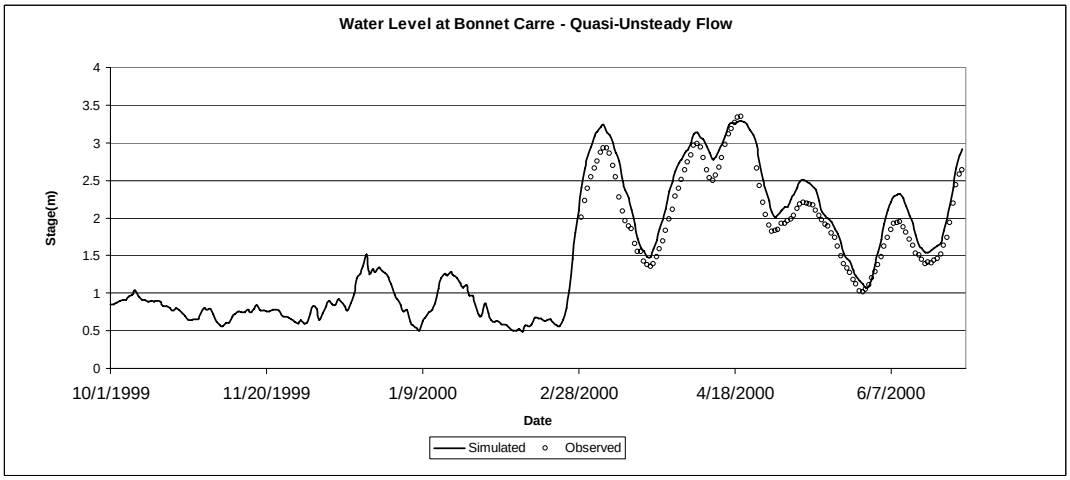

Figure 26: Observed/Simulated Stage at Bonnet Carré, Quasi-Unsteady Flow 1999/00

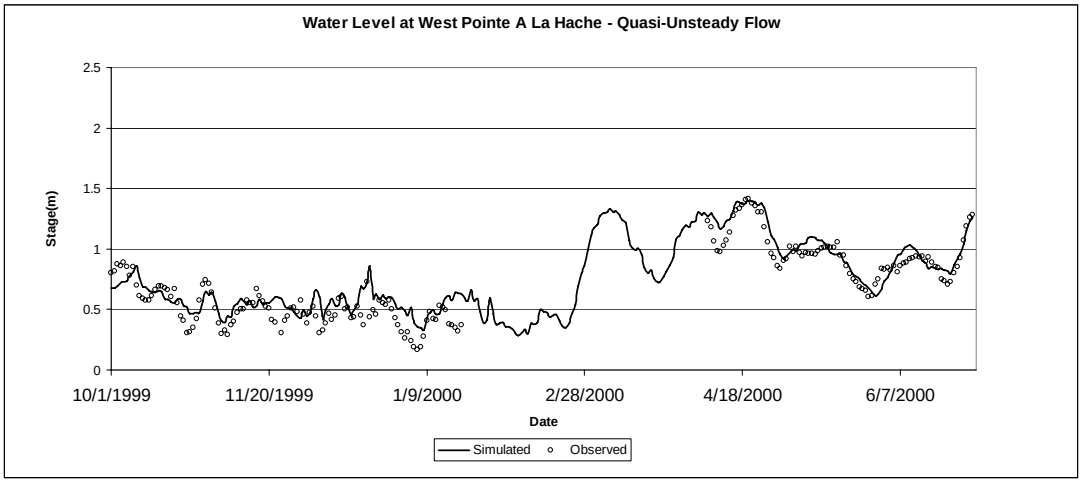

Figure 27: Observed/Simulated Stage at Pointe a La Hache, Quasi-Unsteady Flow 1999/00

Statistical summary of the model performance for the validation period is shown below in Table 10. As evident from Figures 24 through 27 and from Table 10, the model compares well against the field measurements.

Table 10: Statistical summary of the model performance for the Validation Period

Location	RMSE (m)	Efficiency
Mississippi River at Red River Landing	0.321	0.964
Mississippi River at Baton Rouge	0.369	0.964
Mississippi River at Bonnet Carre	0.256	0.798
Mississippi River at West Pointe A La Hache	0.117	0.836

After the hydrodynamics had been calibrated and validated, effort was directed to calibrate the sediment module for the Lower Mississippi River. Field data available at Belle Chase were compared with the model results for the period of 1978/79. Annual estimated sand loads at Belle Chasse were obtained based on the available discrete measurements. The calibration was initially performed with the Ackers-White sediment transport and the Toffaleti fall velocity formulas. Other sediment transport formulas were also tested. Overall, among all the methods tested, Engelund-Hansen gave favorable results compared to the field measurements. Therefore, further model calibration was performed utilizing the Engelund-Hansen sediment discharge predictor.

Three water years were used to validate the model: 1977/78, 1979/80 and 1992/93. The annual sand loads calculated by the model varied between around 50% and 165% of the estimated annual load based on field data. Estimated and simulated annual sand loads for Belle Chasse station are shown in Table 11.

Table 11: Estimated versus Modeled - Annual Sand Load at Belle Chasse

WATER YEAR	ESTIMATED SUSPENDED SAND (TONS)	MODELED		Modeled/Estimated
		FORMULA	SUSPENDED SAND (TONS)	
1977/78	13,983,927	Engelund-Hansen	9,134,578	65%
1978/79	32,542,279	Engelund-Hansen	33,090,920	102%
1979/80	20,518,654	Engelund-Hansen	9,859,757	48%
1992/93	16,007,443	Engelund-Hansen	26,258,640	164%

Considering the scarcity of the field data and the challenges associated with sediment transport predictions, the results presented in Table 11 are reasonable, as the error does not exceed a factor of 2. It is well documented in the literature that sediment load estimates between 200% and 50% of the measurements are acceptable (Van Rijn (1982) and White et al. (1973).

Logarithmic plots of the relation between sand load and water flow were prepared for both the field observations and the model predictions. The comparison between the observed and modeled values can be seen in Figures 28 through 31. It is evident that the model is more efficient in predicting the sand transport under high concentrations occurring during higher flows.

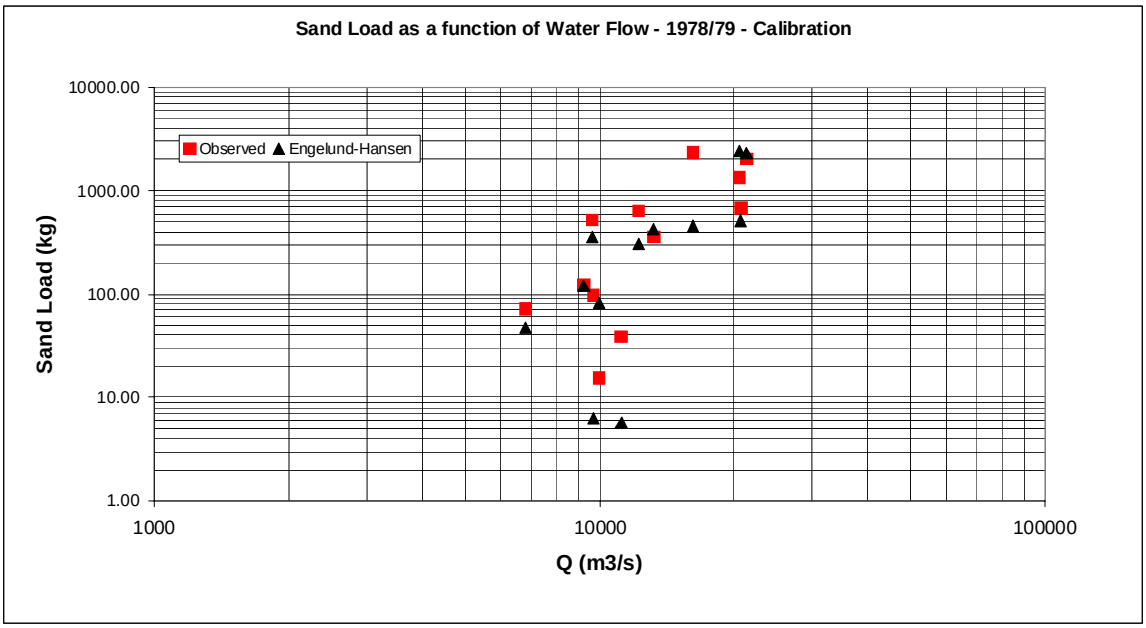

Figure 28: Observed/Simulated Sand Load as a function of Water Flow, Calibration period of 1978/79
Results obtained with Engelund-Hansen formula. Site: Belle Chasse.

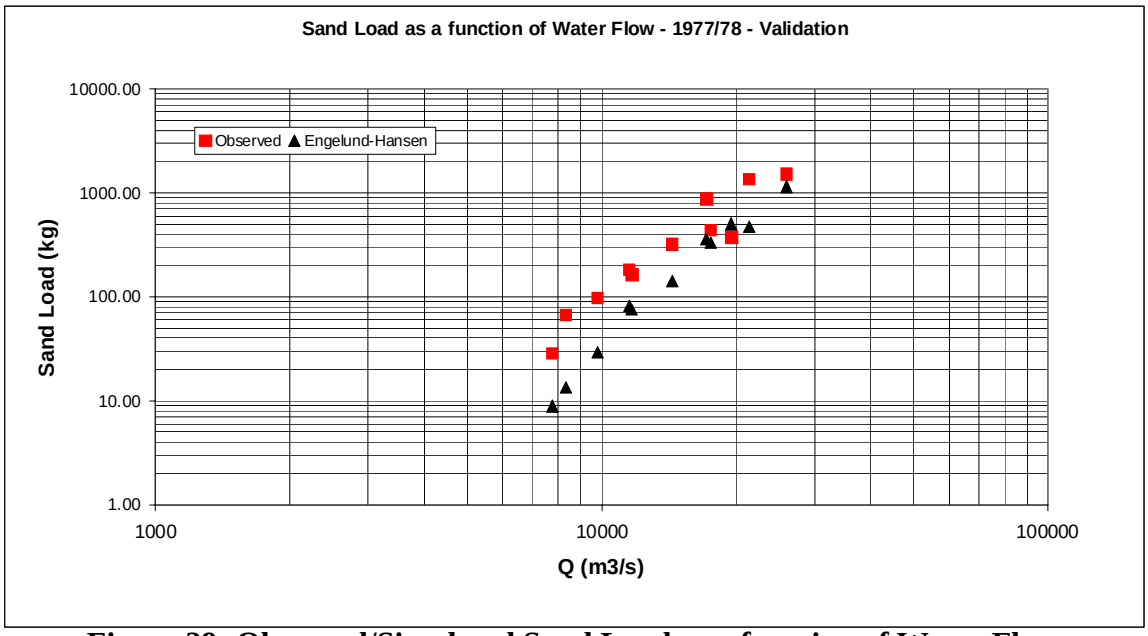

Figure 29: Observed/Simulated Sand Load as a function of Water Flow, Validation period of 1977/78

Results obtained with Engelund-Hansen formula. Site: Belle Chasse.

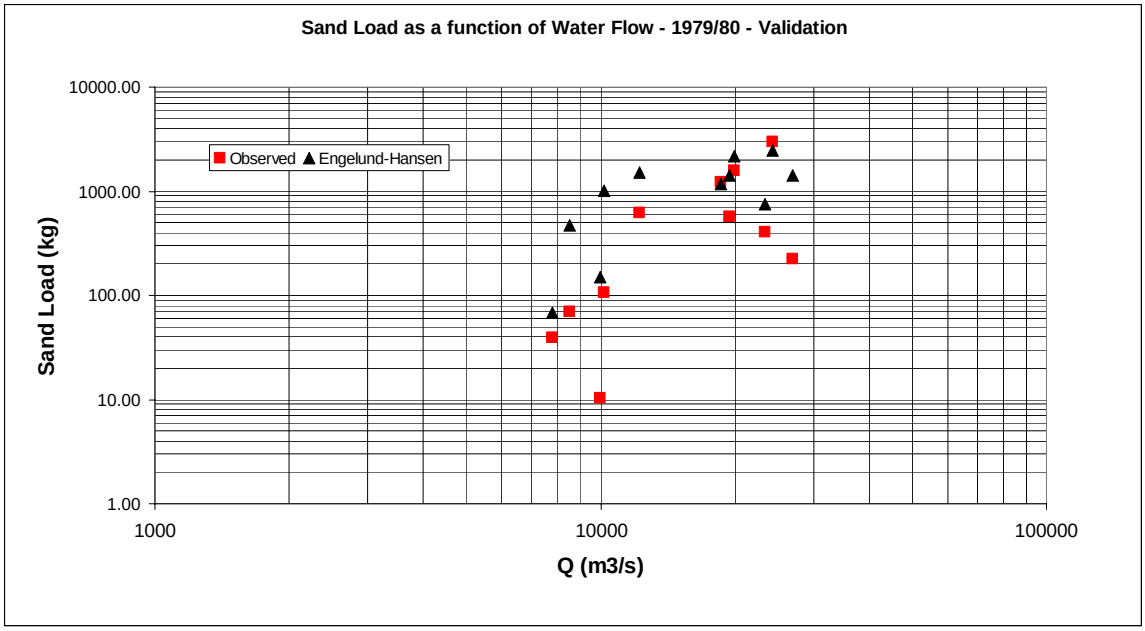

Figure 30: Observed/Simulated Sand Load as a function of Water Flow, Validation period of 1979/80

Results obtained with Engelund-Hansen formula. Site: Belle Chasse.

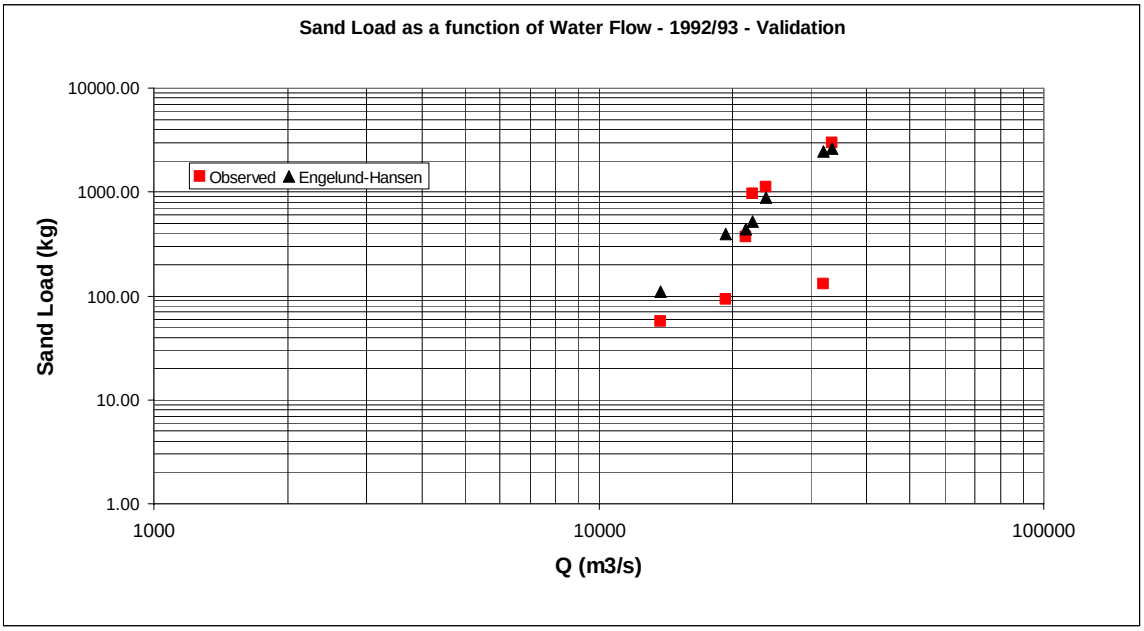

Figure 31: Observed/Simulated Sand Load as a function of Water Flow, Validation period of 1992/93
Results obtained with Engelund-Hansen formula. Site: Belle Chasse.

To further validate the sediment module, additional simulations for the drought period of 1999 to 2000 were performed to assess the model's ability to predict the erosion and migration rates of the earthen sill constructed by the U.S. Army Corps of Engineers.

The 1999-2000 mobile-bed simulations included tests with 5 different sediment transport formulas:

- Ackers-White
- Engelund-Hansen
- Yang
- Toffaleti
- Laursen

Engelund-Hansen sediment predictor provided more realistic results in comparison with the other formulas. Figure 32 shows the thalweg variations at the top of the earthen sill during the simulated period. As shown in the figure, the HEC-RAS model was capable of reproducing the erosion pattern reflected in the field measurements. The model slightly underestimated the extent of the erosion though.

Longitudinal bed profiles measured in February and May 2000 are shown in Figure 33. The migration and the erosion of the sill top are evident from these two profiles. The HEC-RAS

prediction of the sill profile in May 2000 is also shown. The HEC-RAS model reproduced both the migration and erosion of the sill top. Again, the model slightly underestimated the erosion and migration processes. However, given the limited data available including the sediment size distribution of the material from which the sill was constructed, the results provided confidence in the model ability to produce reliable predictions.

5.5 Assessment of Dredging the Borrow Areas

Once the HEC-RAS was calibrated and validated for both hydrodynamics and sediment transport, additional simulations were performed to assess the impact of dredging MR-B-09 and MR-E-09. Potential impact from the dredging operation may include head-cutting, shoaling, and scour; those impacts might occur locally, upstream, or downstream from the dredging site.

Two simulations were performed to examine the potential impact of the dredging operation December 2007 to June 2008 (a period that includes an extreme flooding event) and January 1999 to December 2000 (representing two years of low and average conditions, respectively).

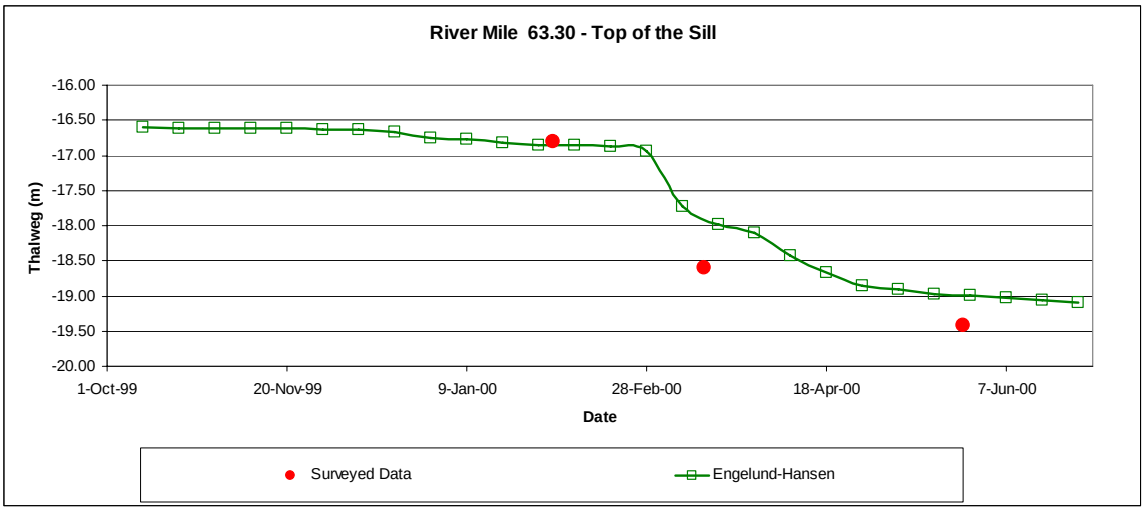

Figure 32: Observed/Simulated thalweg variation obtained with Engelund-Hansen formula

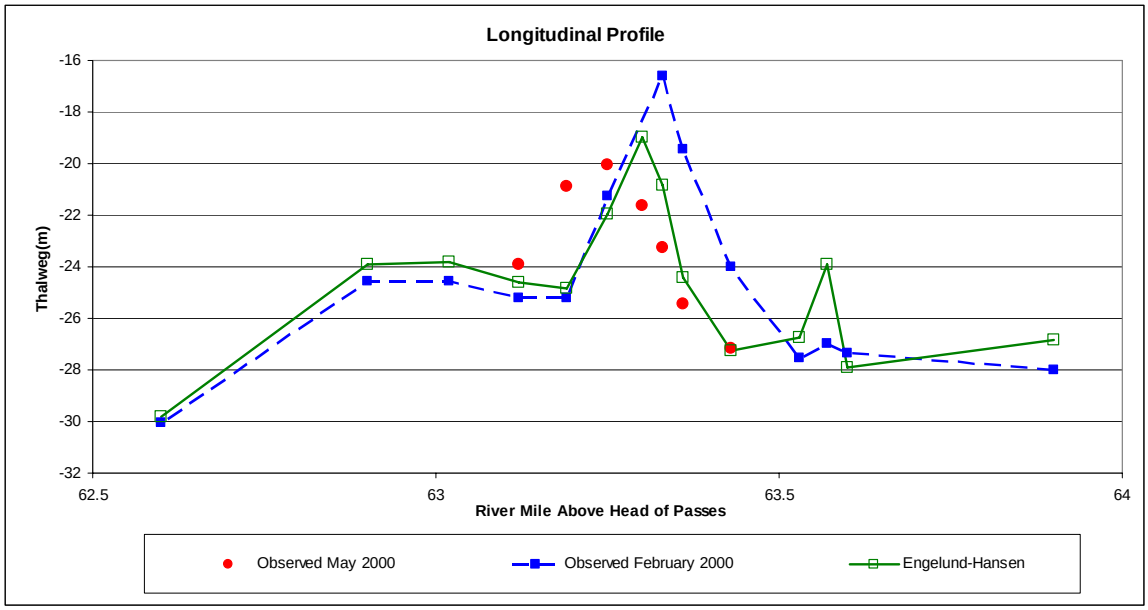

Figure 33: Observed/Simulated Longitudinal Profile of the Sill obtained with Engelund-Hansen formula

For the December 2007 to June 2008 period, discrete water discharge and sediment load at Belle Chasse and water level (stage) at Venice were used as boundary conditions. The characterization of the bottom material was based on the field measurements conducted in January and April of 2008. The ratio of the sand bed-load to sand suspended load was used to estimate the total sand load at Belle Chasse. Figure 34 shows the estimated total sand load used as the boundary condition at Belle Chasse.

Figure 35 shows the simulated and measured water level at West Point a La Hache, while figures 36 and 37 show the simulated and measured water level at the two stations installed within the project area (MM 24.2 and MM 16), respectively. The monitoring stations at MM 24.2 and MM 16 are referred to as Scofield North and Scofield South, respectively. Overall, the model results compare well against the field measurements. As mentioned earlier, the quasi-unsteady numerical simulations were performed with daily time step. These unavoidable restrictions with the HEC-RAS version 4.0 model results in some discrepancies between the field measurements and the model predictions. However, it was observed that the model results captured the overall trend and therefore provided a reliable assessment of the dredging operation.

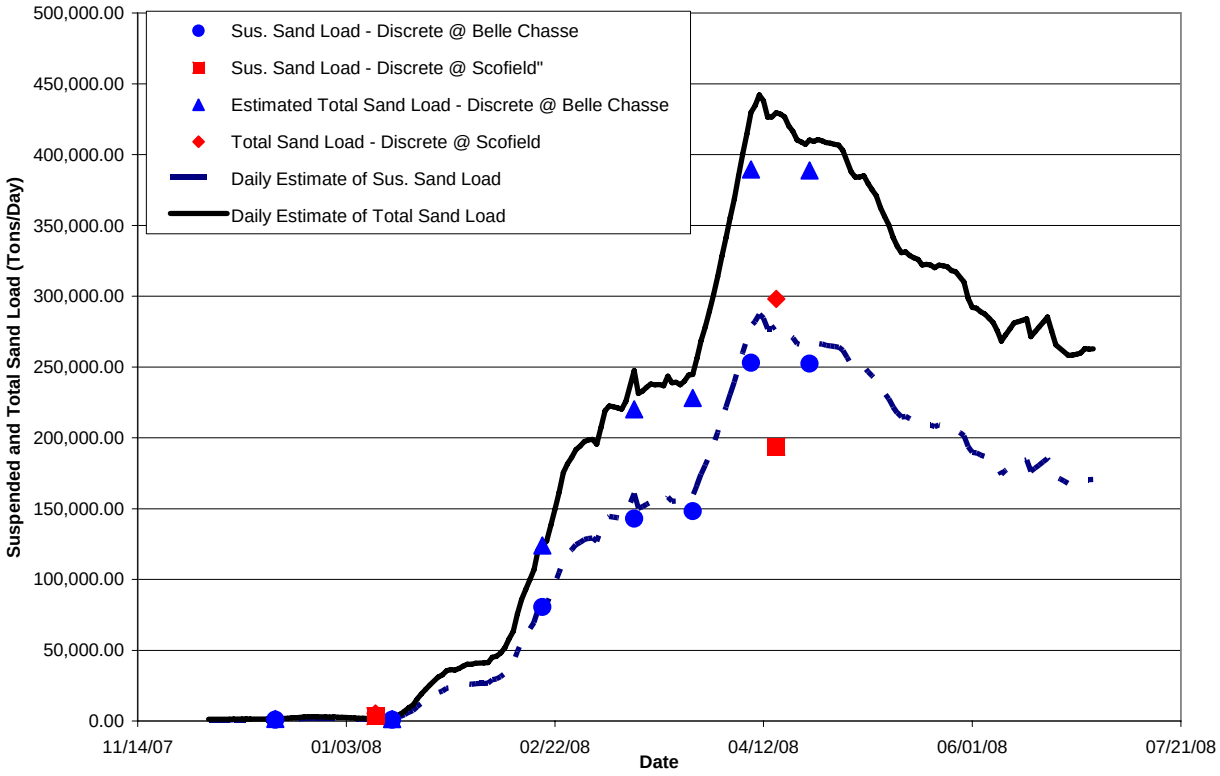

Figure 34: Estimated total sand load at Belle Chasse (MM 76).
Suspended and total sand load measured at MM 30 (Scofield) are also shown

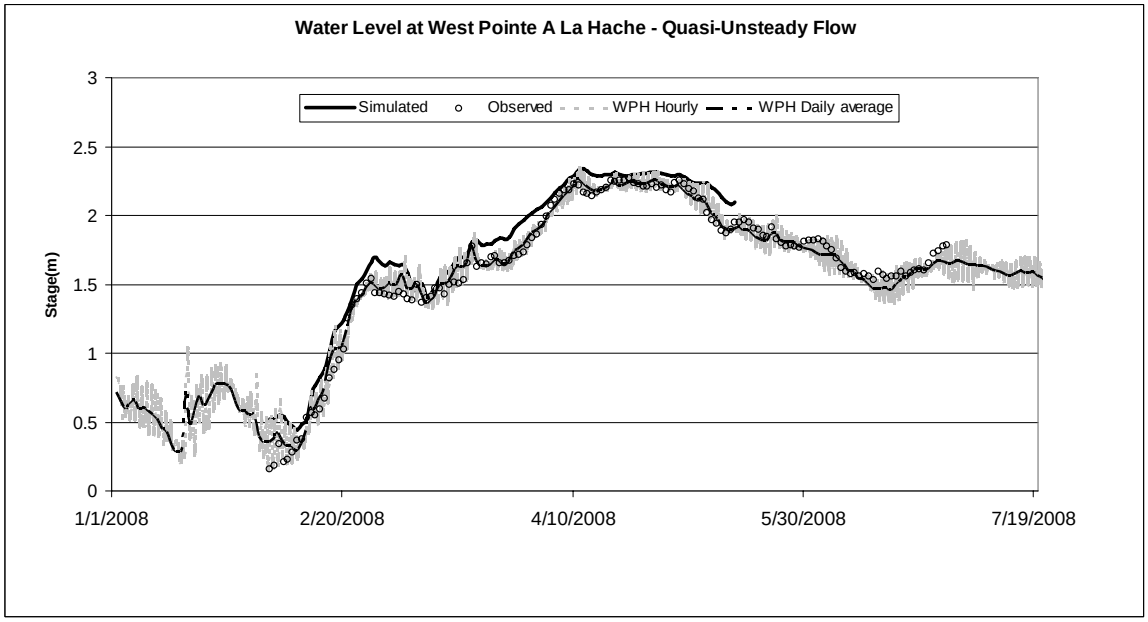

Figure 35: Simulated/Measured stage at West Point a La Hache

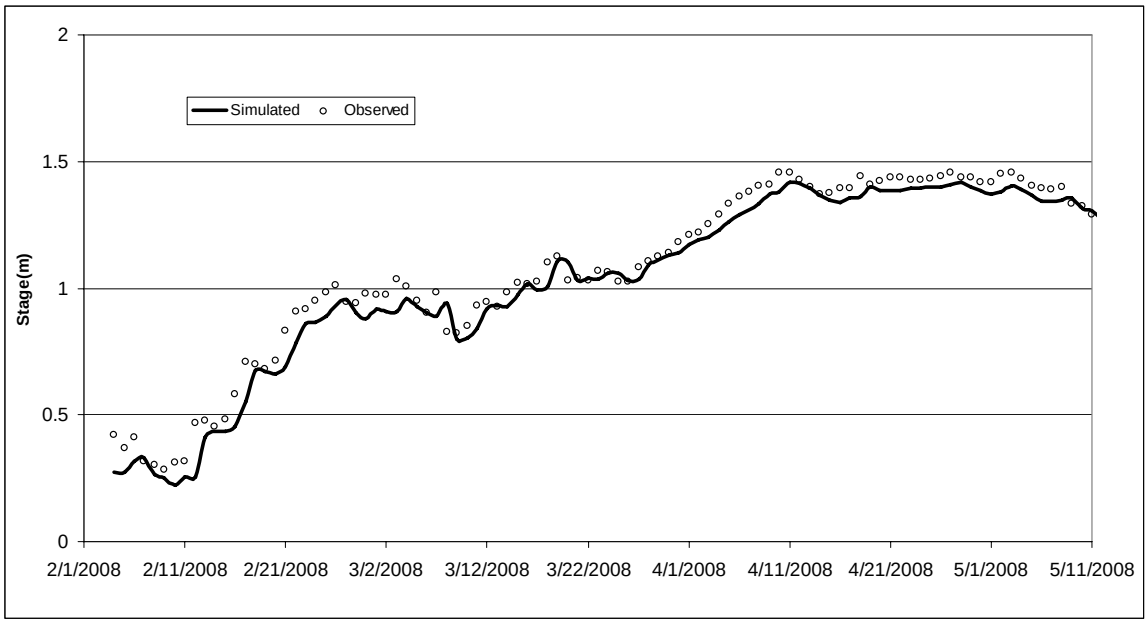

Figure 36: Simulated/Measured stage at Scofield North (MM 24.2)

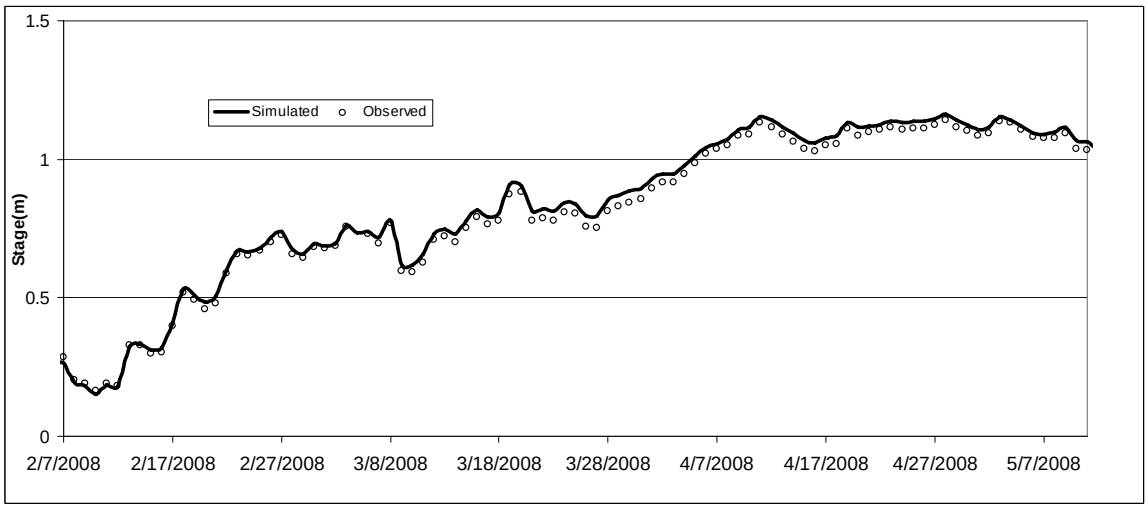

Figure 37: Simulated/Measured stage at Scofield South (MM 16)

Table 12 shows the measured and simulated sand concentration in mg/L at the project site for January and April of 2008. The HEC-RAS results compared well with the measurements for the high flow event of April 2008. The measurements indicated that there was no sand load at low flow. As listed in Table 12, HEC-RAS predicted very small, although not exactly zero, sand load during the January 2008 time period.

Table 12: Simulated/Measured and sand concentration for January and April 2008

Date	Concentration (mg/L)							
	Measured	Simulated						
		Engelund-Hansen		Ackers-White		Toffaletti		
		Scofield-North	Scofield-South	Scofield-North	Scofield-South	Scofield-North	Scofield-South	
1/10/2008	0.00	9.56	10.30	8.03	8.52	16.72	17.88	
4/15/2008	71.02	83.15	67.74	111.64	108.84	72.87	72.00	

Two new geometry files were created in HEC-RAS each reflecting the footprint of one of the borrow areas. A plan view of the HEC-RAS cross-sections that were modified to reflect the dredging of MR-B-09 and MR-E-09 is shown in Figure 38.

To assess the impact of dredging each borrow area, three simulations were performed; one with no dredging (Base Run), a second with only Borrow Area MR-B-09 dredged, and a third with only Borrow Area MR-E-09 dredged. The excavation limits were matched with those evaluated in the Feasibility Study (SJB and CEC, 2008). A dredge depth of 70 feet below the water surface was chosen corresponding to the approximate limits of the dredge plant anticipated to be utilized for Project construction. This yielded approximate volumes of 8.5 million cubic yards and 5.8 million cubic yards for MR-B-09 and MR-E-09, respectively. As previously stated, the decision was made to perform the numerical simulations under these conservative conditions to assess potential dredging impacts under the "worst case" scenario.

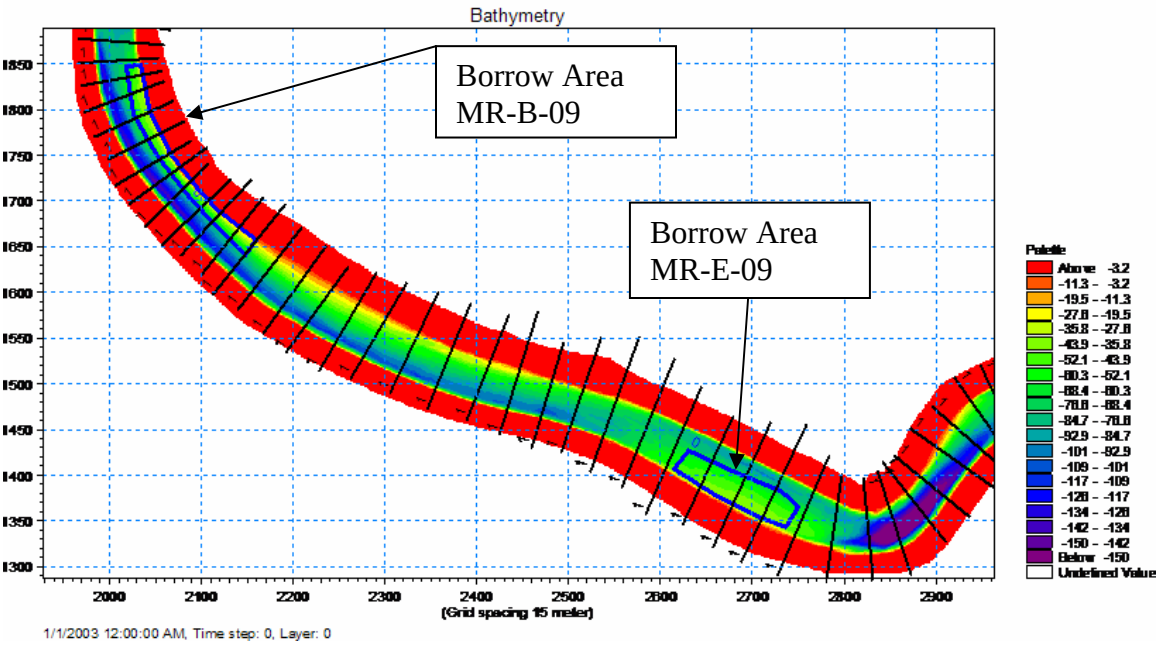

Figure 38: Plan view of the HEC-RAS cross-sections

Figure 39 shows the thalweg profile from MM 31 to 21 above head of passes for the Base Run and MR-B-09. The limits of each borrow area is shown along the profile. Figure 40 shows thalweg profiles for the Base Run and MR-E-09. The same analysis was repeated again with the 1999 to 2000 simulation. Figures 41 and 42 show a comparison between the thalweg profiles for the Base Run versus MR-B-09 and MR-E-09, respectively.

It is also important to investigate the temporal evolution of the river bottom at and in the vicinity of the borrow areas to understand the morphological stability and to examine any potential impact on the levee stability control lines. Figures 43 through 46 show the cumulative change of mass of the river bottom at a given cross-section. Positive change indicates deposition while negative change indicates erosion. The four figures are for changes within the limits of MR-B-09, downstream of MR-B-09, within the limits of MR-E-09, and upstream of MR-E-09, respectively. Finally to assess the impact of the dredging on the average flow velocity, hydrographs of the flow velocities at the same locations mentioned above are presented in Figures 47 through 50.

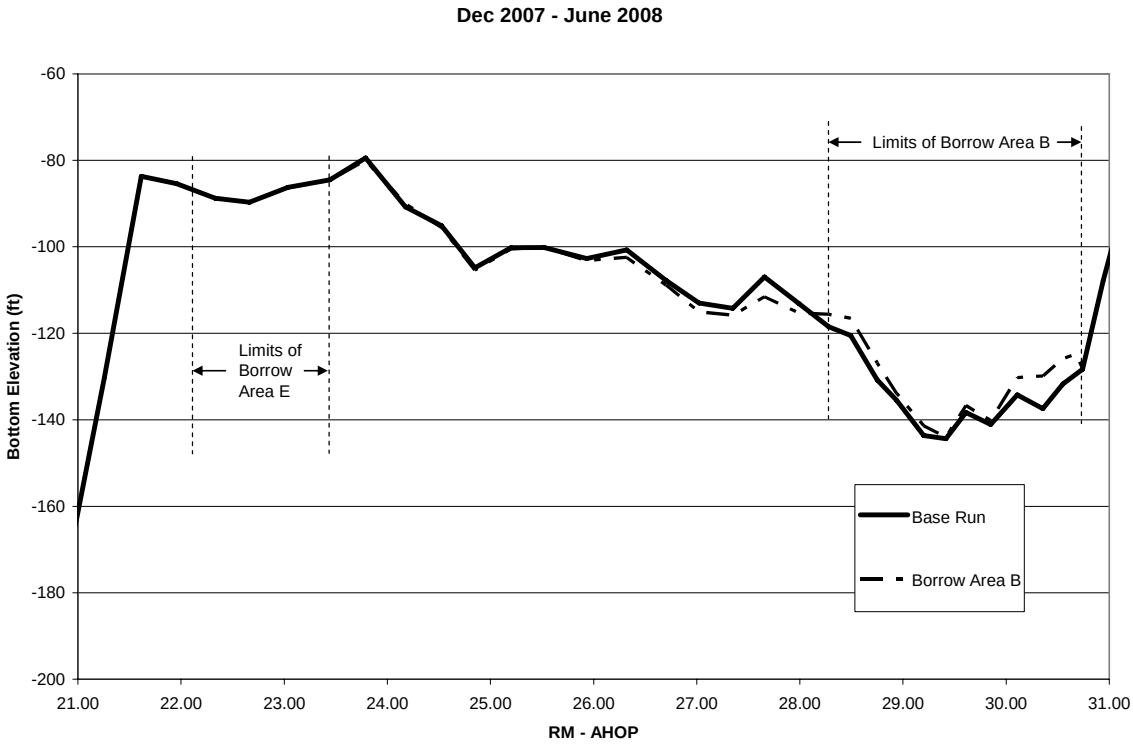

Figure 39: Thalweg profiles for the Base Run and MR-B-09

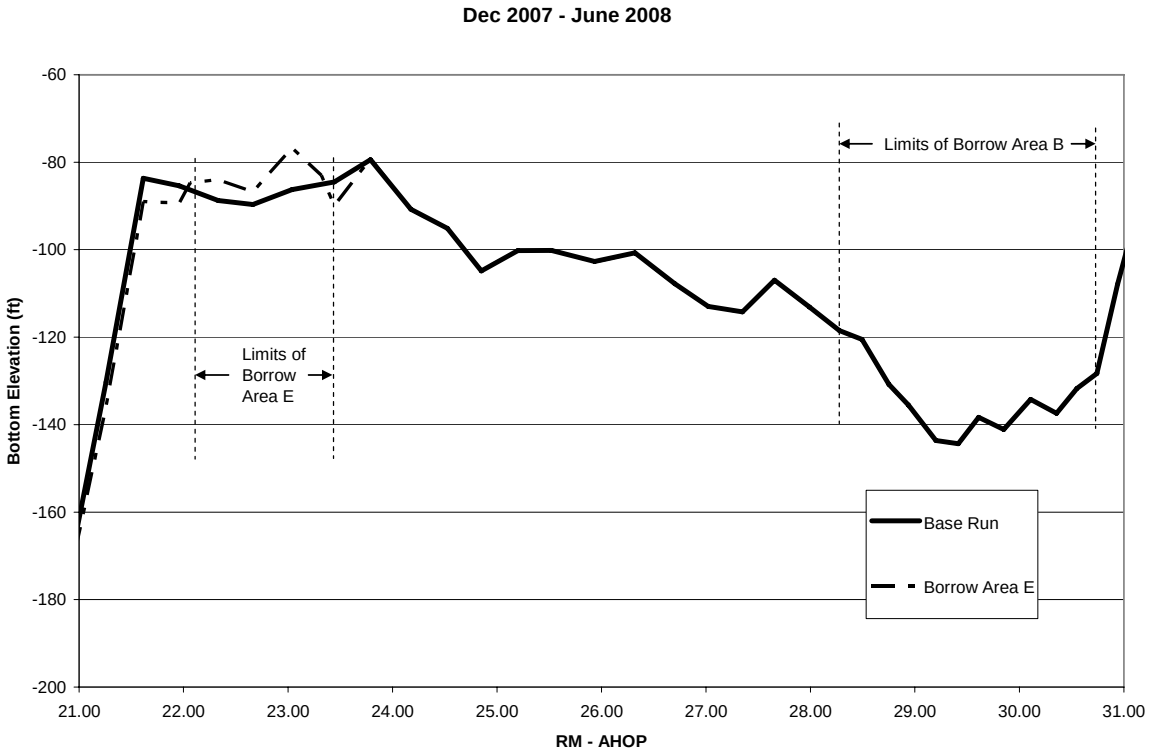

Figure 40: Thalweg profiles for the Base Run and MR-E-09

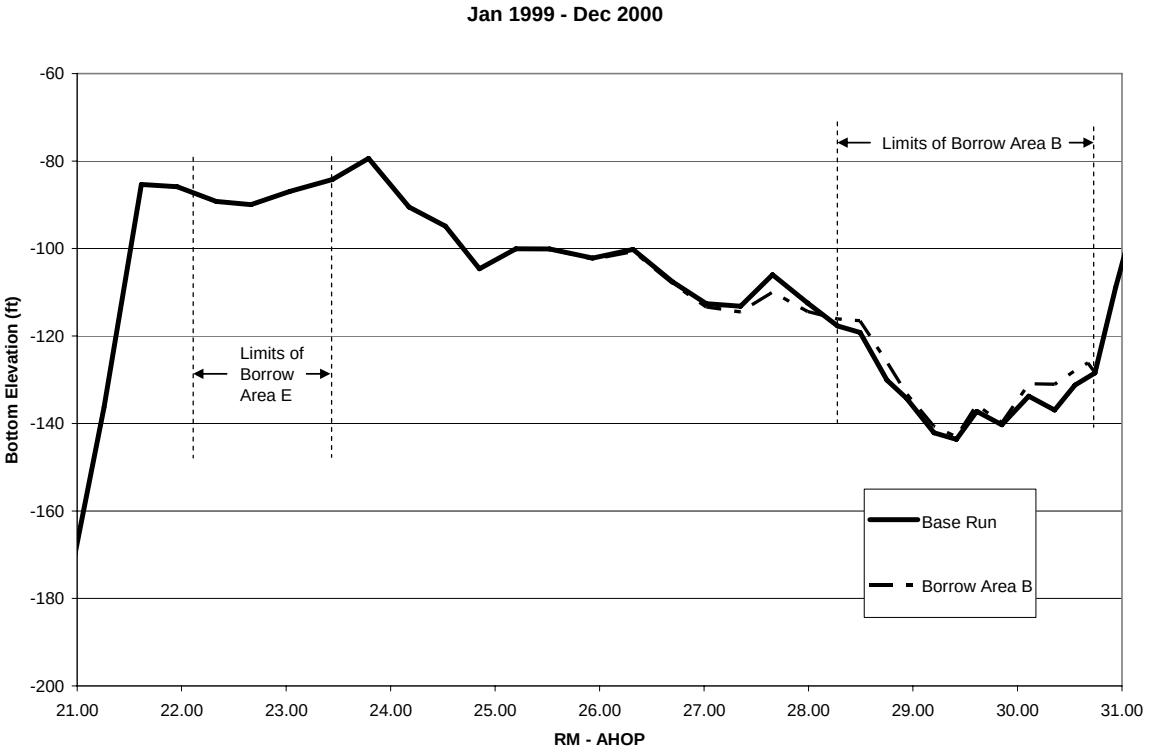

Figure 41: Thalweg profiles for the Base Run and MR-B-09

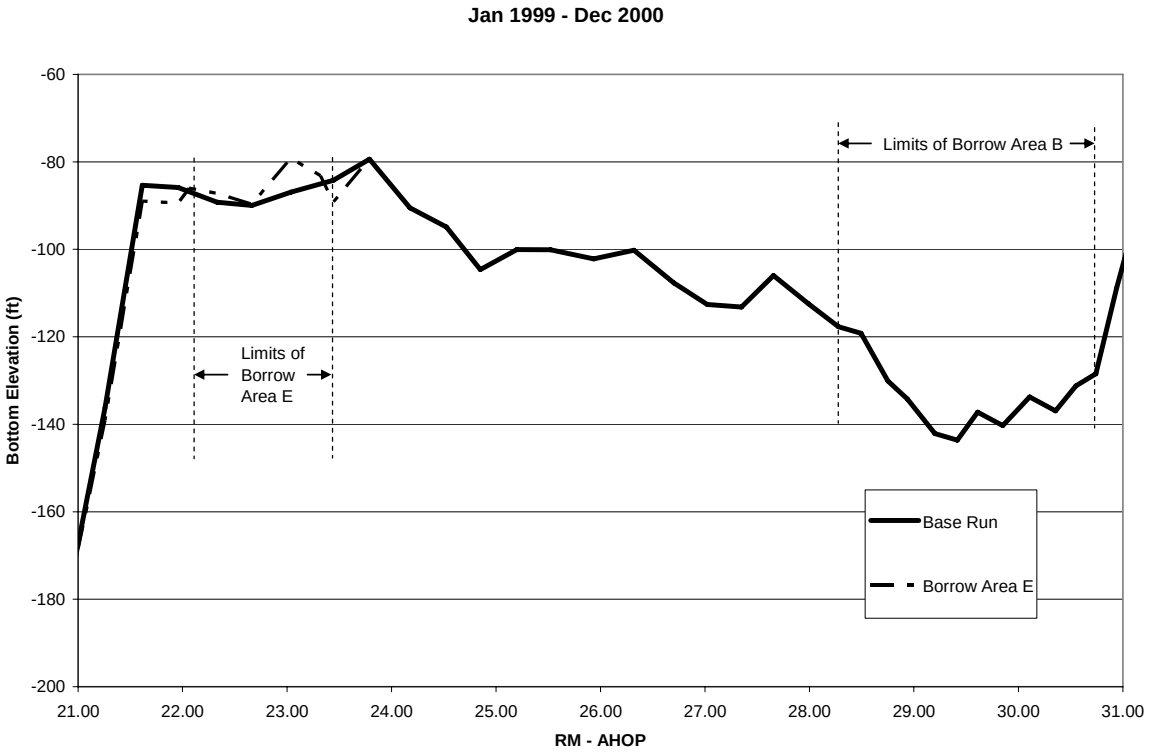

Figure 42: Thalweg profiles for the Base Run and MR-E-09

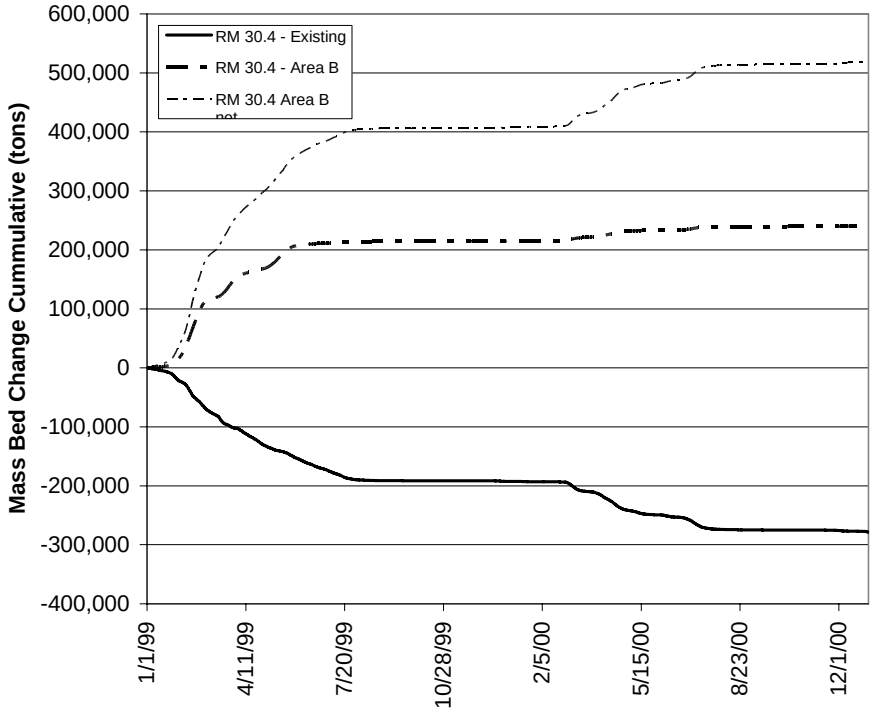

Figure 43: Cumulative mass bed change within the Limits of MR-B-09

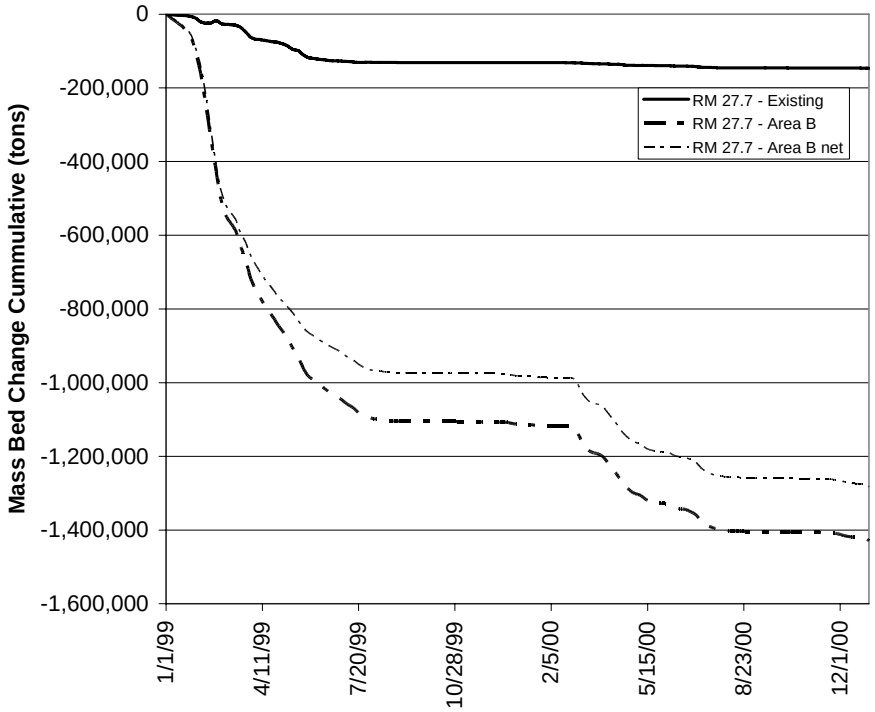

Figure 44: Cumulative mass bed change downstream of MR-B-09

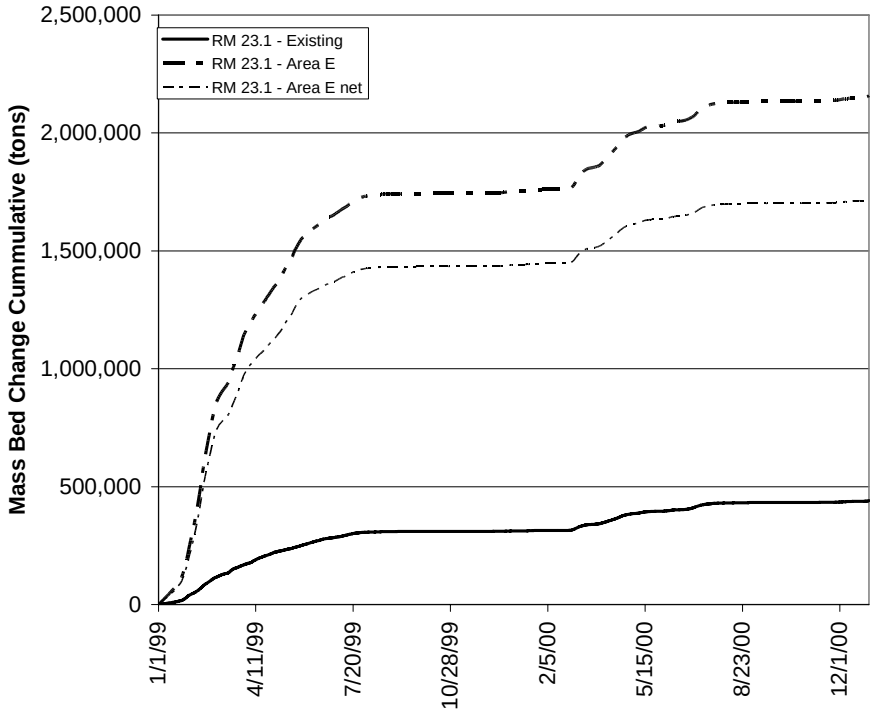

Figure 45: Cumulative mass bed change within the Limits of MR-E-09

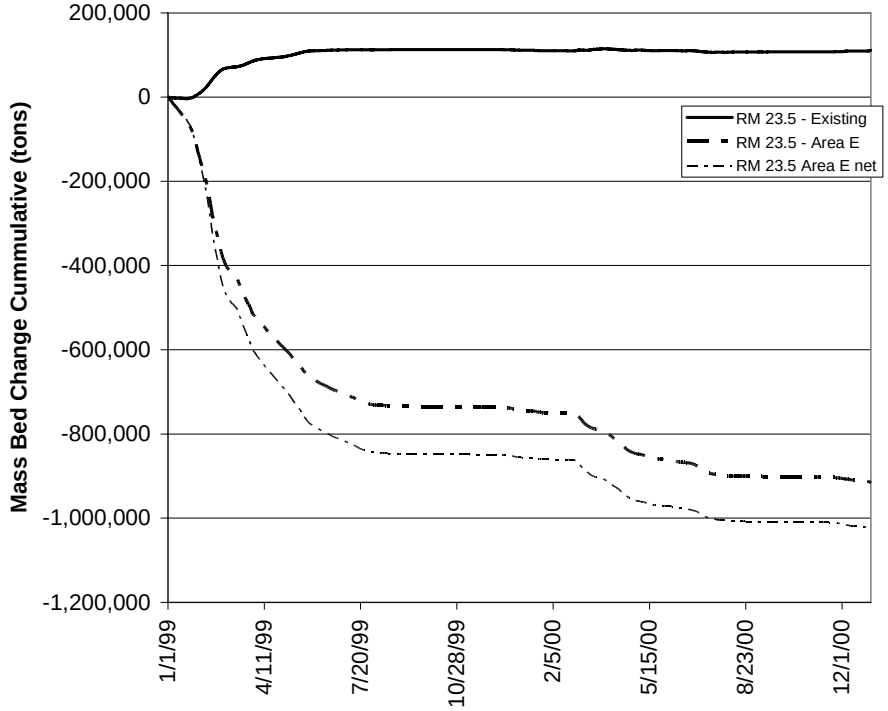

Figure 46: Cumulative mass bed change upstream of MR-E-09

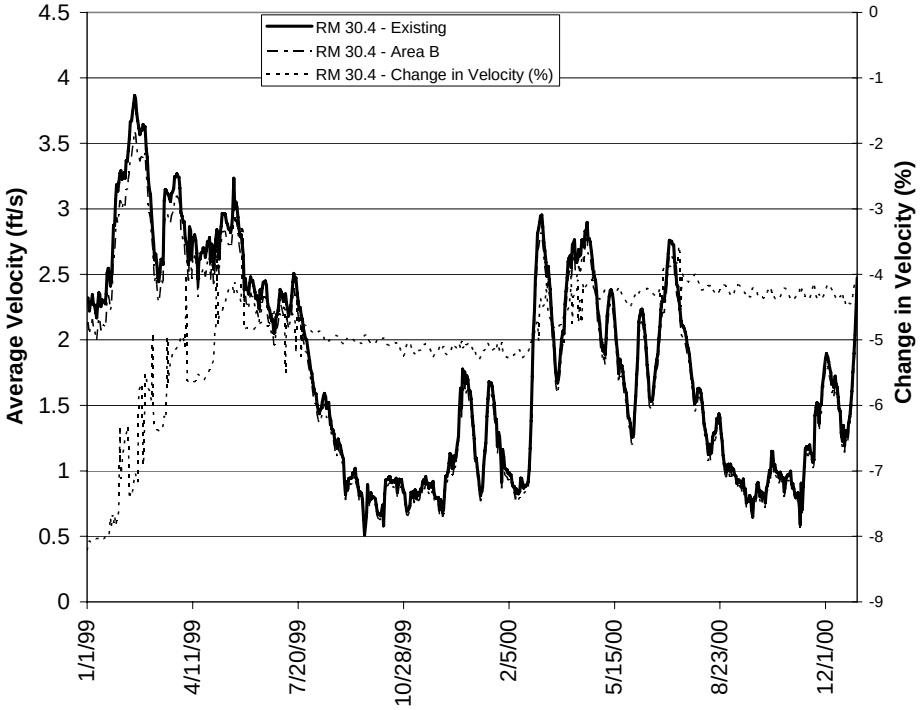

Figure 47: Average velocity within the limits of MR-B-09 for the Base Run

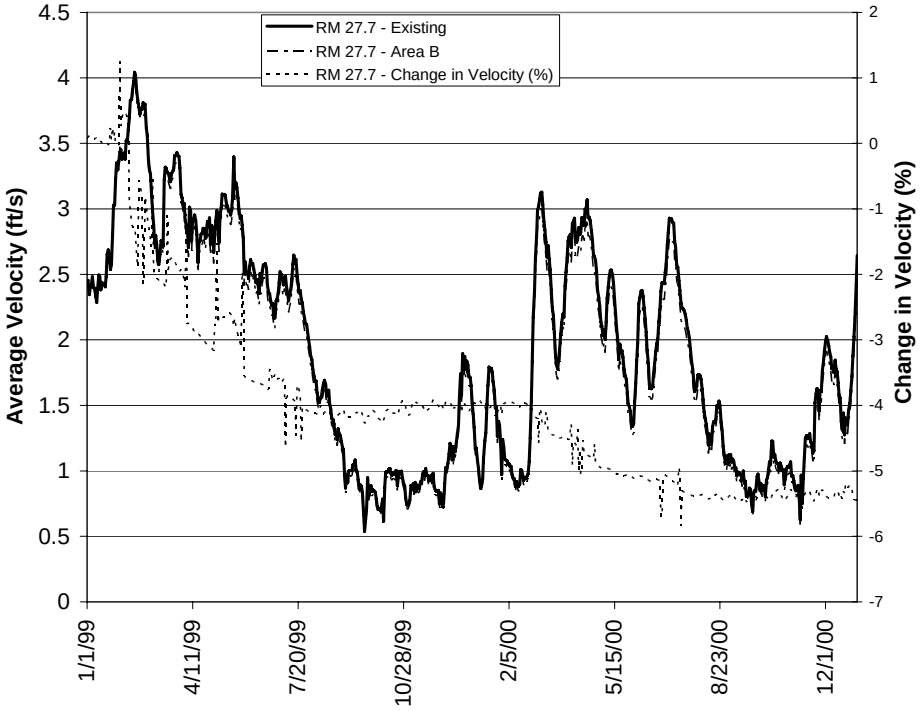

Figure 48: Average velocity downstream of MR-B-09 for the Base Run

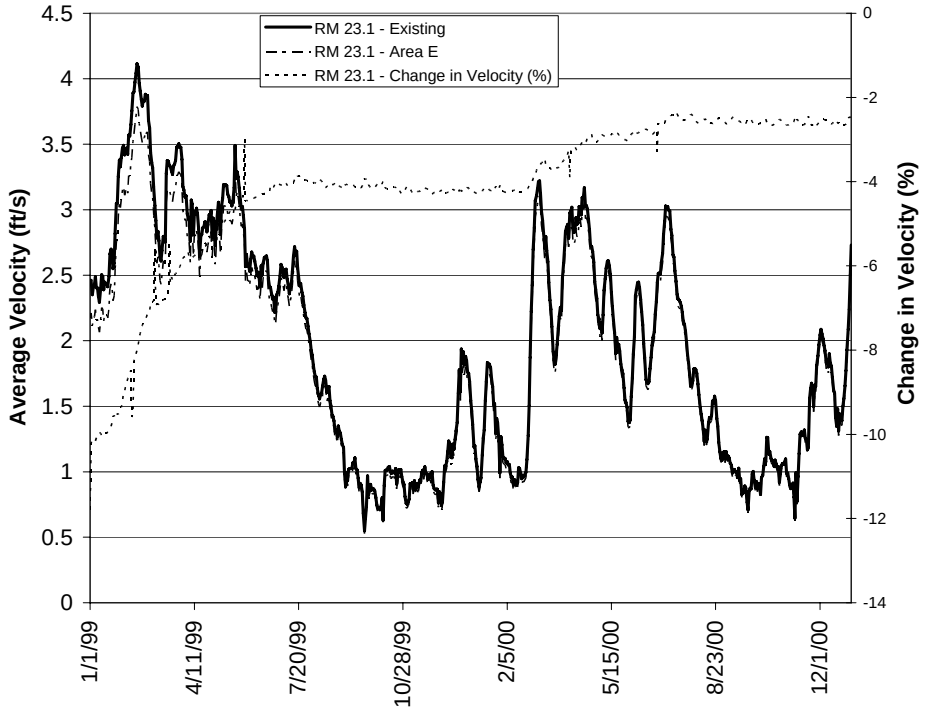

Figure 49: Average velocity within the limits of MR-E-09 for the Base Run

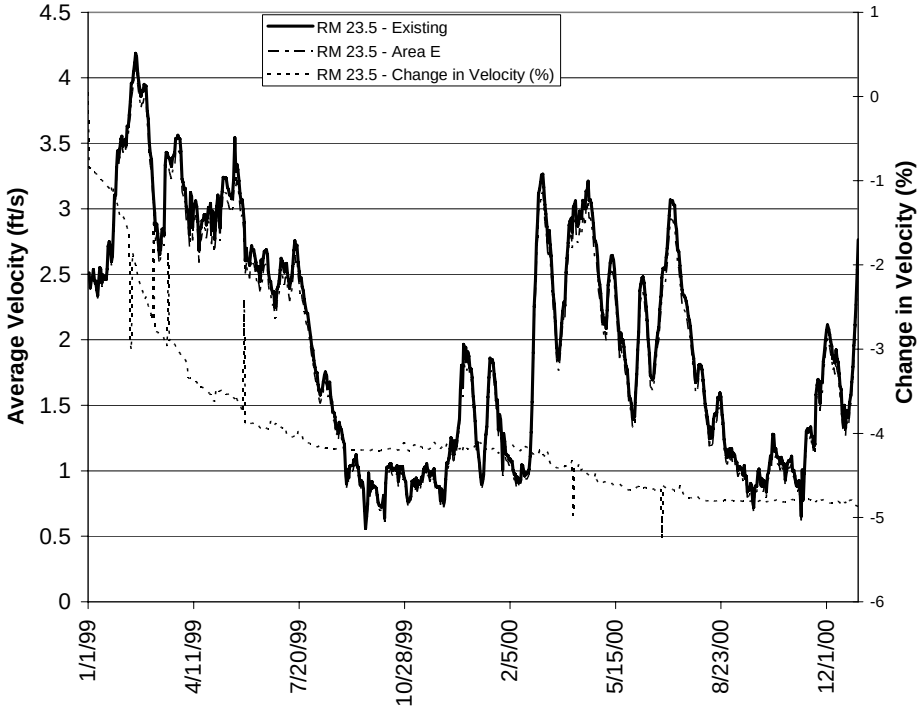

Figure 50: Average velocity upstream of MR-E-09 for the Base Run

5.6 Discussions and Recommendations

As seen from the results presented above, local deposition was predicted at both borrow areas. It was also noted that erosion was predicted to occur downstream of both borrow areas but was contained within a short distance of 0.5 to 1 mile in each case. The results also showed minor erosion taking place upstream (head-cutting) of MR-E-09. Thus, it is evident that dredging of either borrow area did not result in or cause excessive head-cutting or erosion. Overall, the bed changes predicted by the HEC-RAS model were in the same order of magnitude as the migrating bed forms in the Lower Mississippi River, therefore they were considered to be within the range of the natural variability experienced by the river due the seasonal changes of the water discharge.

The model results also showed that immediately after dredging a borrow area, the average velocity decreased within the limits of each borrow area by approximately 10%, then as the borrow areas started to fill up, the change in velocity declined to less than 5% within 2 years. The model results also showed that, toward the end of the two-year simulation, immediately upstream and downstream of the borrow areas, the change in average velocity approached 5% of the velocities of the Base Run.

The numerical model results showed that both borrow areas exhibit similar responses to dredging. However, it should be noted the one-dimensional model provided total quantities of erosion and deposition; i.e. spatial transverse distribution cannot be inferred. Moreover, the one-dimensional numerical model did not provide quantitative pictorials of local hydraulics at the river bends.

In summary, excavation of the two borrow areas yielded subtle changes in river hydrodynamics on the same order of magnitude as natural variability in the river. The model results provide reasonable assurance that mining these borrow areas will not result in negative impacts to river hydrodynamics. Based on the modeling results, it was concluded there was no need to perform two- or three-dimensional numerical modeling analyses to further assess the potential impacts of dredging MR-B-09 or MR-E-09.

6.0 REFERENCES

Ackers, Peter and White, William R. 1973. Sediment Transport: New Approach and Analysis, *Journal of Hydraulics Division*, Vol. 99, No. HY11, pp. 2041-2060, American Society of Civil Engineers (ASCE).

Allison, M. 2008. Field Studies Notes, January and April.

Belo, J.C. 1992. Modelacao Matematica de Escoamentos Variaveis com leito Movel, Dissertacao de Mestrado, *Instituto Superior Tecnico*, Lisboa.

Chen, C., Beardsley, R. G. and Cowles, G. 2006. An Unstructured Grid, Finite-Volume Coastal Ocean Model – FVCOM User Manual, Marine Ecosystem Dynamics Modeling Laboratory (MEDM) Version 2.5, Second Edition, June.

Christopher Goodwin & Associates, Inc. 2008. Phase I Marine Archeological Remote Sensing Survey of the Proposed Mississippi River Sand Borrow Sites for the Louisiana Coastal Area Barrier Shoreline Restoration Project, Plaquemines Parish, Louisiana (DRAFT). Submitted to U.S. Army Corps of Engineers, New Orleans District.

Coastal Planning & Engineering. 2004. Technical Assessment of Riverine Sand Mining to Support Scofield Island Restoration. Submitted to National Oceanic and Atmospheric Administration (NOAA) National Marine Fisheries Service.

Finkl et al., C.W., J.L. Andrews, L. Benedet, and T. Campbell. 2005. Geotechnical Investigation for Exploration of Sand Resources in the Lower Mississippi River and South Pass, and Exploration for Sand via Vibracoring in South Pelto Blocks 12 & 13. Boca Raton Florida:

Coastal Planning & Engineering, Inc. 40p. Report Prepared for the Louisiana Department of Natural Resources, Baton Rouge, Louisiana.

Laursen, E. M. 1958. The Total Sediment Load of Streams, Paper 1530, *Journal of the Hydraulics Division - Proceedings of the American Society of Civil Engineers*, February.

SJB Group, LLC and C. H. Fenstermaker and Associates, Inc. 2007. Mississippi River Mining Impact Assessment Technical Memorandum, Task A.4.3 Riverine Sand Mining / Scofield Island Restoration (BA-40). LDNR Contract No. 2511-07-02, Technical Memorandum A.4.3. Submitted to Louisiana Department of Natural Resources, Coastal Engineering Division.

SJB Group, LLC and Coastal Engineering Consultants, Inc. 2007a. Transport Methodology and Access Corridors Technical Memorandum, Riverine Sand Mining / Scofield Island Restoration (BA-40). LDNR Contract No. 2511-07-02, Technical Memorandum A.4.1. Submitted to Louisiana Department of Natural Resources, Coastal Engineering Division.

SJB Group, LLC and Coastal Engineering Consultants, Inc. 2007b. Mississippi River Mining Technical Memorandum, Riverine Sand Mining / Scofield Island Restoration (BA-40). LDNR Contract No. 2511-07-02, Technical Memorandum A.4.2. June 27, 2007. Submitted to Louisiana Department of Natural Resources, Coastal Engineering Division.

SJB Group, LLC and Coastal Engineering Consultants, Inc. 2007c. Mississippi River Mining Technical Memorandum, Riverine Sand Mining / Scofield Island Restoration (BA-40). LDNR Contract No. 2511-07-02, Technical Memorandum B.5.1 & B.5.2. October 17, 2007. Submitted to Louisiana Department of Natural Resources, Coastal Engineering Division.

SJB Group, LLC and Coastal Engineering Consultants, Inc. 2008. Draft Feasibility Study Report. Mississippi River Riverine Sand Mining / Scofield Island Restoration (BA-40). LDNR Contract No. 2511-07-02. March 10, 2008. Submitted to Louisiana Department of Natural Resources, Coastal Engineering Division.

White, R., Milli, H. and Crabbe, A. D. 1973. Sediment Transport: An Appraisal of Available Methods, Volume 1 – Summary of Existing Theories, *Report No IT 119, Hydraulics Research Station Wallingford*, November.

White, R., Milli, H. and Crabbe, A. D. 1973. Sediment Transport: An Appraisal of Available Methods, Volume 2 – Performance of Theoretical Methods when Applied to Flume and Field Data, *Report No IT 119, Hydraulics Research Station Wallingford*, November.

Mellor, G.L. 2003. Users Guide for a Three-Dimensional Primitive Equation, Numerical Ocean Model, Program in Atmospheric and Ocean Sciences, Princeton University.

Meselhe, E. A., Habib, E., Griborio, A. G., Gautam, S., McCorquodale, J. A. and Georgiou, I. Y. 2005. Hydro-Ecological Modeling of Lower Mississippi River, Proceedings of the 14th Biennial Coastal Zone Conference, New Orleans, LA, July.

Toffaleti, F. B. 1969. Definitive Computations of Sand Discharge in Rivers, *Journal of the Hydraulics Division*, Vol. 95, No. HY1, pp. 225-248, American Society of Civil Engineers (ASCE).

USACE. 1993. HEC-6, Scour and Deposition in Rivers and Reservoirs, User's Manual, USACE Hydrologic Engineering Center, August.

USACE. 2002. HEC-RAS River Analysis System - Hydraulic Reference Manual Version 3.1, USACE Hydrologic Engineering Center, November.

USACE. 2006. HEC-RAS River Analysis System - User's Manual Version 4.0 Beta, USACE Hydrologic Engineering Center, November.

USACE. 2008. HEC-RAS River Analysis System - User's Manual Version 4.0, USACE Hydrologic Engineering Center: http://www.hec.usace.army.mil/software/hec-ras/, March.

Van Rijn, L. C. 1984. Sediment Transport, Part I: Bed Load Transport, *Journal of Hydraulic Engineerin*g, American Society of Civil Engineers, Vol. 110, No. 10, pp 1412-1430

Van Rijn, L. C. 1993. Principles of Sediment Transport in Rivers, Estuaries, Coastal Seas and Oceans, International Institute for Infrastructural, Hydraulic and Environmental Engineering, Delft, the Netherlands